Bioscience Reports (2018) **38** BSR20171350
https://doi.org/10.1042/BSR20171350

PORTLAND PRESS

Research Article

Genome-wide differential expression profiling of mRNAs and lncRNAs associated with prolificacy in Hu sheep

Xu Feng, Fengzhe Li, Feng Wang, Guomin Zhang, Jing Pang, Caifang Ren, Tingting Zhang, Hua Yang, Ziyu Wang and Yanli Zhang

Jiangsu Livestock Embryo Engineering Laboratory, Nanjing Agricultural University, Nanjing 210095, China

Correspondence: Yanli Zhang (zhangyanli@njau.edu.cn)

OPEN ACCESS

Reproductive ability, especially prolificacy, impacts sheep profitability. Hu sheep, a unique Chinese breed, is recognized for its high prolificacy (HP), early sexual maturity, and year-round estrus. However, little is known about the molecular mechanisms underlying HP in Hu sheep. To explore the potential mRNAs and long non-coding RNAs (lncRNAs) involved in Hu sheep prolificacy, we performed an ovarian genome-wide analysis of mRNAs and lncRNAs during the follicular stage using Hu sheep of HP (litter size = 3; three consecutive lambings) and low prolificacy (LP, litter size = 1; three consecutive lambings). Plasma luteinizing hormone (LH) concentration was higher in the HP group than in the LP group ($P<0.05$) during the follicular stage. Subsequently, 76 differentially expressed mRNAs (DE-mRNAs) and five differentially expressed lncRNAs (DE-lncRNAs) were identified by pairwise comparison; quantitative real-time PCR (qRT-PCR) analysis of ten randomly selected DE genes (mRNA and lncRNA) were consistent with the sequencing results. Gene Ontology (GO) analysis of DE-mRNAs revealed significant enrichment in immune response components, actin filament severing and phagocytosis. Pathway enrichment analysis of DE-mRNAs indicated a predominance of immune function pathways, including phagosomes, lysosomes, and antigen processing. We constructed a co-expression network of DE-mRNAs and mRNA-lncRNAs, with *C1qA*, *CD53*, cathepsin B (*CTSB*), *CTSS, TYROBP*, and *AIF1* as the hub genes. Finally, the expression of lysosomal protease cathepsin genes, *CTSB* and cathepsin D (*CTSD*), were significantly up-regulated in sheep ovaries in the HP group compared with the LP group ($P<0.05$). These differential mRNAs and lncRNAs may provide information on the molecular mechanisms underlying sheep prolificacy.

Introduction

Reproductive ability has important impacts on the profitability of sheep production. Reproduction is a complex process, and traits such as ovulation rate and litter size are genetically affected by causative mutations in some minor and major genes [1,2]. Hu sheep is a local breed in China with high prolificacy (HP), year-round estrus, and an average litter size of 2.06. Approximately 17.35% of these sheep have one lamb, while 17.61% have three lambs. Thus, knowledge of the genes involved in ovulation rate and litter size, and their effects, provides useful information for Hu sheep breeding and for the selection of these traits [3]. To date, mutations in bone morphogenetic protein 15 (*BMP15*), growth differentiation factor 9 (*GDF9*), and bone morphogenetic protein receptor, type 1B (*BMPR-1B*) have been identified in some sheep breeds as fecundity genes that affect follicular development and ovulation [4]. However, mutations in these fecundity genes have different effects on ovulation rate and litter size. For example, *BMP15* has a limited effect on the fecundity

Received: 09 October 2017
Revised: 30 January 2018
Accepted: 31 January 2018

Accepted Manuscript Online: 08 February 2018
Version of Record published: 27 April 2018

© 2018 The Author(s). This is an open access article published by Portland Press Limited on behalf of the Biochemical Society and distributed under the Creative Commons Attribution License 4.0 (CC BY).

Bioscience Reports (2018) **38** BSR20171350
https://doi.org/10.1042/BSR20171350

of Hu sheep and Merino sheep, but it has a clear effect on the fecundity of Small Tail Han sheep [3,5]. Therefore, it is necessary to identify other major genes affecting Hu sheep prolificacy.

Non-coding RNAs (ncRNAs) play vital roles in eukaryotic gene regulation. Long non-coding RNA (lncRNAs) are greater than 200 nts in length, represent one of the most highly expressed ncRNAs in animals, and regulate the expression of neighboring coding genes [6]. In animals, the level of lncRNA expression is lower than that of normal coding genes, but has more functions than we knew before. Based on its position in the genome, lncRNA can be divided into five categories: divergent lncRNA, sense lncRNA, antisense lncRNA, intergenic lncRNA, and intronic lncRNA [7]. Because of their different modes of action and origin, they are mainly involved in life processes, such as X-chromosome inactivation, chromatin remodeling, histone modification, transcription regulation, and post-transcriptional regulation in the organism [8-11]. In recent years, researchers have focussed on the role of lncRNA in early animal germ cell formation, early embryo implantation and development, and hormone regulation in human and animal reproduction [12-14]. The cumulus cells around bovine oocytes transport large amounts of nutrients and substances, including mRNA and lncRNA, to the oocytes [15]. Furthermore, similar studies in mice have also found that ovarian somatic cells transfer RNA and other cytoplasmic substances into the oocyte, including lncRNA. [16-18]. The lncRNA nuclear paraspeckle assembly transcript 1 (*Neat1*) was found to be essential for corpus luteum formation, and for the establishment and maintenance of female pregnancy in animals [19]. A recent study also showed that the differential regulation of miRNAs and lncRNAs might be related to fecundity in Small Tail Han sheep and Dorset sheep [20]. Despite these findings, research on prolificacy-associated lncRNA in Hu sheep and its target mRNA, especially their interaction networks, remains limited.

In the present study, we compared the patterns of reproductive hormones and *BMPR-1B* mutations in Hu sheep with high and low prolificacy (LP), and then used strand-specific RNA sequencing (ssRNA-seq) to identify the role of mRNAs and lncRNAs in sheep ovaries during this process. We identified genome-wide differentially expressed mRNAs (DE-mRNAs) and lncRNAs (DE-lncRNAs) in each comparison, and Gene Ontology (GO) and Kyoto Encyclopedia of Genes and Genomes (KEGG) enrichment analyses of DE-mRNAs and target genes of lncRNAs were conducted. We further constructed mRNA–mRNA and lncRNA–mRNA regulatory networks associated with sheep prolificacy.

Materials and methods

Animals and sample collection

All experimental procedures were conducted in strict compliance with the recommendations of the Guide for Animal Experiments of Nanjing Agricultural University, China (approval ID: SYXK2011-0036).

Ewes with three lambing records were divided into two groups: an HP group (n=4, litter size = 3) and an LP group (n=4, litter size = 1). Animals were raised at the Taizhou Hailun Sheep Industry Co., Ltd (Jiangsu, China) under similar conditions with free access to feed and water. First, we conducted synchronous estrus before the experiment, a vaginal sponge was implanted for 11 days, followed by the administration of 0.2 mg cloprostenol at the time of sponge removal. Estrus was tested by the ram at 9 a.m., 12 noon, and 6 p.m. each day. After the first estrus was detected, blood was collected from the jugular vein at 9 a.m. every morning, and the ewes were used for intensive blood collection prior to slaughter, when they were confirmed to be in estrus. All blood samples were treated with heparin sodium for anticoagulation and centrifuged at 3000 rpm for 15 min to separate the plasma, which was then stored at −20°C. After slaughter, all left ovary samples were immediately collected and stored at −80°C for total RNA extraction.

Polymorphism analysis of BMPR-1B

To determine the type of mutation in the *BMPR-1B* gene in the HP and LP groups, blood was collected from all the ewes. Exon 6 (741–936 bp) of *BMPR-1B* was amplified. Primer sequences are provided in Supplementary Table S1. PCR was performed in a 40-μl volume containing approximately 20 pmol primer. Amplification conditions were as follows: initial denaturation at 94°C for 5 min; followed by 35 cycles of denaturation at 94°C for 30 s, 60°C for 30 s, extension at 72°C for 30 s; with a final extension at 72°C for 7 min using a T100 Thermal Cycler (Bio–Rad, U.S.A.). The sense strand of the amplified product was subsequently sequenced.

ELISA

Serum levels of estradiol (E2), follicle stimulating hormone [21], and luteinizing hormone (LH) were assayed using ELISA. Frozen serum samples were thawed slowly at room temperature, along with the assay kits (Kmaels, China, E2: #DRE-S9105c, FSH: #DRE-S0622c, LH: #DRE-S5741c). Samples, standards, and HRP-labeled detection antibodies

© 2018 The Author(s). This is an open access article published by Portland Press Limited on behalf of the Biochemical Society and distributed under the Creative Commons Attribution License 4.0 (CC BY).

were sequentially added to the coated microwells precoated with sheep hormones capture antibody, incubated and washed thoroughly. Tetramethyl benzidine (TMB) was converted into blue by peroxidase catalysis and the final yellow color under acidic conditions. The absorbance (OD value) was measured with a microplate reader at a wavelength of 450 nm to calculate the concentration of hormones. All assays were performed according to the manufacturer's protocol in duplicate.

RNA extraction, library construction, and RNA-seq

Total RNA was extracted from ovaries using TRIzol reagent (Invitrogen, Carlsbad, CA). RNA concentration and purity were measured using the NanoDrop 2000 spectrophotometer (Thermo Fisher Scientific, Wilmington, DE). RNA integrity was assessed using the RNA Nano 6000 Assay Kit of the Agilent Bioanalyzer 2100 System (Agilent Technologies, CA, U.S.A.). In total, 1.5 μg RNA per sample was used as the input material for rRNA removal using the Ribo-Zero rRNA Removal Kit (Epicentre, Madison, WI, U.S.A.).

Sequencing libraries of six samples (HP group, n=3; LP group, n=3) were generated using NEBNextR Ultra^{TM} Directional RNA Library Prep Kit for IlluminaR (NEB, U.S.A.) following the manufacturer's recommendations, and index codes were used to label the sequences of each sample. To select fragments of 150–200 bp, the library fragments were purified with AMPure XP Beads (Beckman Coulter, Beverly, U.S.A.). Then, 3 μl USER Enzyme (NEB, U.S.A.) was used with size-selected, adaptor-ligated cDNA at 37°C for 15 min before PCR. Then, PCR was performed with Phusion High-Fidelity DNA polymerase, Universal PCR primers and Index (X) Primer. Finally, PCR products were purified (AMPure XP system, Beckman Coulter, Beverly, MA, U.S.A.) and library quality was assessed on the Agilent Bioanalyzer 2100 and via quantitative real-time PCR (qRT-PCR). Index-coded samples were clustered on acBot Cluster Generation System using TruSeq PE Cluster Kitv3-cBot-HS (Illumia) according to the manufacturer's instructions. After cluster generation, the library preparations were sequenced on an Illumina Hiseq platform and then paired-end reads were generated.

Read mapping and lncRNA prediction

Raw data (raw reads) in fastq format were processed through in-houseperl scripts. In this step, clean data (clean reads) were obtained by removing reads containing adapters, reads containing poly-N, and low-quality reads from raw data. At the same time, Q20, Q30, GC-content, and sequence duplication of the clean data were calculated. All downstream analyses were based on high-quality clean data. The transcriptome was assembled using Cufflinks (version 2.1.1) and Scripture based on reads mapped to the *Ovis aries* reference genome (Oar_v3.1). The assembled transcripts were annotated using the Cuffcompare program from the Cufflinks package. Unknown transcripts were used to screen for putative lncRNAs. Four computational approaches, including the coding potential calculator (cpc), coding-non-coding index (cnci), protein families database (pfam), and coding-potential assessment tool (cpat) [22-25], were combined to sort non-protein-coding RNA candidates from putative protein-coding RNAs in the unknown transcripts.

Putative protein-coding RNAs were filtered using a minimum length and exon number threshold. Transcripts with lengths exceeding 200 nts, and with more than two exons, were selected as lncRNA candidates, and were further screened using cpc/cnci/pfam/cpa, which can distinguish protein-coding from non-coding genes. Then, the different types of lncRNAs, including lincRNA, intronic lncRNA, and antisense lncRNA, were selected using cuffcompare. Cuffdiff (version 2.1.1) was used to calculate fragments per kilobase of exon per million fragments mapped (FPKMs) of coding genes and lncRNAs in each sample [26]. Gene FPKMs were computed by summing the FPKMs of transcripts in each gene group.

Based on the mode of lncRNA action on target genes, we used two predictive methods. First, lncRNA regulates the expression of neighboring genes, which can be predicted based on the position of lncRNA and mRNA, and adjacent genes within a range of 100 kb of its target gene. Second, lncRNA and mRNA function through base pairing, and the LncTar [27] target gene prediction tool was used to predict the target gene of lncRNA.

Differential expression analysis and gene functional annotation

Differential expression analysis of DE-mRNA and DE-lncRNA in the two groups was performed using the DESeq R package (1.10.1). DESeq provides statistical routines to determine differential gene expression within digital data using a model based on the negative binomial distribution. The resulting P-values were adjusted using the Benjamini and Hochberg approach to control the false discovery rate (FDR). Genes with an adjusted FDR < 0.05 and absolute value of $\log_2$ (fold change) >1 found by DESeq were classed as being differentially expressed. Gene function was

© 2018 The Author(s). This is an open access article published by Portland Press Limited on behalf of the Biochemical Society and distributed under the Creative Commons Attribution License 4.0 (CC BY).

Bioscience Reports (2018) **38** BSR20171350
https://doi.org/10.1042/BSR20171350

annotated based on the following databases: Nr, Pfam, Swiss-Prot, KEGG, GO. GO enrichment analysis of the differentially expressed genes (DE-mRNAs) was implemented by the topGO (R package, version 2.8) R package. We used KOBAS [28] software to test the statistical enrichment of differentially expressed genes in the KEGG pathways.

Construction of mRNA–mRNA and lncRNA–mRNA networks

To infer the function of DE-lncRNA and DE-mRNAs in sheep prolificacy, we constructed a complementary pair network based on mRNA and mRNA as well as between mRNA and lncRNA, by using cytoscape (V3.4.0).

Validation of gene expression of by qRT-PCR

For the qRT-PCR analysis, 1 μg total RNA was reverse transcribed using RT reagent kits with gDNA Eraser (Takara, China) according to the manufacturer's protocol. Real-time PCR was performed on an ABI 7300 (Applied Biosystems, Foster City, CA, U.S.A.) with Fast Start Universal SYBR Green Master (ROX) (Roche, Mannheim, Germany). The following program was used: 95°C for 5 min, followed by 40 cycles at 95°C for 10 s, 60°C for 30 s, and 72°C for 30 s. Primers for mRNAs and lncRNAs are shown in Supplementary Table S1. Glyceraldehyde-3-phosphate dehydrogenase (GAPDH) was used as an internal reference to normalize target gene expression. All experiments were performed in triplicate.

Immunohistochemistry assay of cathepsin B and cathepsin D

Ovaries of ewes were fixed in 4% paraformaldehyde, then embedded in paraffin. Paraffin sections were dewaxed in xylene and subsequently gradually hydrated by gradient alcohol, finally transferred to water. The dewaxed sections incubated with 3% H_2O_2 at 37°C for 15 min to quench the endogenous peroxidase, and antigen retrieval was carried out in citrate buffer solution at 100°C for 15 min. After cooling down to room temperature, the sections were blocked by 5% BSA at 37°C for 30 min; then incubated the sections at 4°C for 12 h with anticathepsin B (#ab125067,abcam, rabbit monoclonal, IgG) and anticathepsin D (#orb180468, Biorbyt, goat polyclonal, IgG) primary antibody. Sections were washed with PBS, then incubated with corresponding secondary antibody and stained by using rabbit IgG SABC immunohistochemical staining kit (#SA2002, Boster Biological Technology Co. Ltd, China) and goat IgG SABC immunohistochemical staining kit (#SA2003, Boster Biological Technology Co. Ltd, China). All sections were examined under microscope (Nikon, Japan).

Statistical analyses

All data are presented as the mean ± S.E.M. When comparisons were made, an independent-sample *t* test was performed using SPSS 24.0 software (SPSS Inc., Chicago, IL, U.S.A.), and $P<0.05$ was considered statistically significant.

Result

Analysis of plasma reproductive hormone concentration and BMPR-1B polymorphism

Plasma E2, FSH, and LH concentrations are shown in Figure 1A. Considering the existence of time variables, we performed repeated measures analysis of covariance (RMANCOVA) to compare the difference in peripheral blood hormone levels between HP ewes and LP ewes. The results show that there were no significant differences in E2 levels during the estrous cycle between HP and LP Hu sheep ($P>0.05$). Additionally, there were no significant differences in the pattern of change in FSH levels between these two groups prior to ovulation ($P>0.05$). However, compared with the LP group before ovulation, the plasma level of LH was significantly higher in the HP group ($P<0.05$).

The mutated sites in BMPR-1B were examined and sequenced (Figure 1B). One genotype, BB, was detected in all the eight ewes. The nucleotide sequence obtained from the BB genotype was identical with that obtained from the wild-type ++, except for an A→G transition at base 746 in the coding region of the *BMPR-1B* gene. This mutation resulted in an amino acid change from glutamine in the wild-type to arginine in the BB genotype (CAG→CGG, Q249R) (Figure 1C).

Transcript assembly and quality control

In total, 238325161 raw paired-end reads were obtained from six samples. In order to test the quality of RNA-seq data, we performed a series of quality control analyses. First, the Q30 of reads in all samples ranged from 93.86 to 94.22%. The average GC content of six libraries was 50.13%. Next, we examined the total coverage of reads from the 5′ to 3′ end of genes. We found that in all samples, RNA-seq reads were evenly distributed, with the exception of the

© 2018 The Author(s). This is an open access article published by Portland Press Limited on behalf of the Biochemical Society and distributed under the Creative Commons Attribution License 4.0 (CC BY).

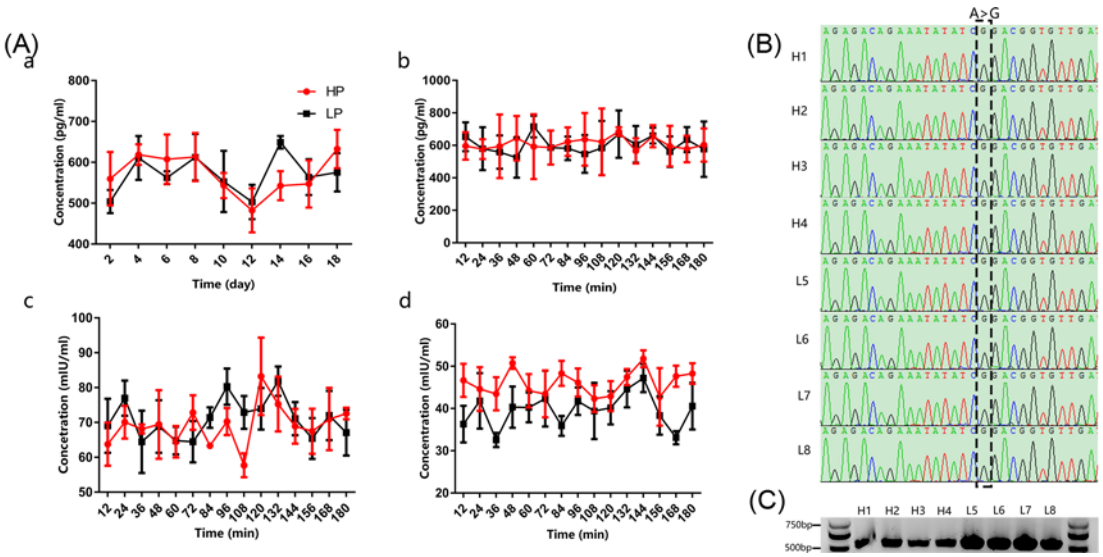

Figure 1. Changes in the concentrations of reproductive hormones and *BMPR-1B* mutations in HP and LP Hu sheep

(**A**) The black and red lines represent data for the HP and LP Hu sheep, respectively. (**a**) Changes in the E2 concentration during the estrous cycle; (**b**) changes in the E2 concentration during intensive blood collection; (**c**) changes in the FSH concentration during intensive blood collection; (**d**) changes in the LH concentration during intensive blood collection. (**B**) Sequencing results for eight ewes. In eight ewes, the CAG site in exon 6 of BMPR-1B amplification products were CGG. (**C**) Representative PCR for the *BMPR-1B* gene performed on samples of every ewe.

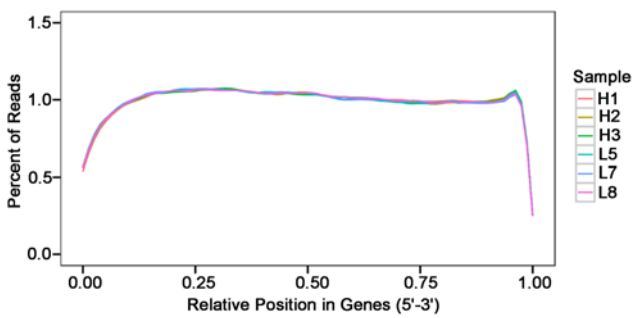

Figure 2. The positional distribution of mapped reads on mRNA

The abscissa is the normalized mRNA position and the ordinate is the percentage of reads in the total range of the corresponding mapped reads. As the length of the reference mRNA differs, each mRNA is divided into 100 intervals by length, and the number and percentage of mapped reads in each interval are counted. The figure summarizes the proportion of mapped reads.

Table 1 Sample quality data assessment statistics

Sample	Obtained reads	Obtained bases (G)	Q30 (%)	GC (%)
H1	41464876	12336861648	94.19	49.87
H2	33523161	9953393728	93.86	49.47
H3	39575613	11747175606	94.07	48.6
L5	42853663	12718293562	94.15	51.23
L7	36307176	10778562464	94.22	51.32
L8	44600672	13235569958	94.09	50.29

Abbreviations: GC (%), sample GC content; Obtained bases, the number of bases obtained; Obtained reads, the number of reads obtained; Q30 (%), percentage of bases with a mass value greater than or equal to 30.

© 2018 The Author(s). This is an open access article published by Portland Press Limited on behalf of the Biochemical Society and distributed under the Creative Commons Attribution License 4.0 (CC BY).

Bioscience Reports (2018) **38** BSR20171350
https://doi.org/10.1042/BSR20171350

Table 2 Sequence comparison of sample sequencing data with the selected reference genome

Sample	Total reads	Mapped reads	Uniq mapped reads	Multiple mapped reads	Reads map to '+'	Reads map to '–'
H1	82929752	67460493 (81.35%)	63602603 (94.28%)	3857890 (5.72%)	34794402 (41.96%)	32666091 (39.39%)
H2	67046322	54271781 (80.95%)	51334082 (94.59%)	2937699 (5.41%)	28090839 (41.90%)	26180942 (39.05%)
H3	79151226	65034922 (82.17%)	61540449 (94.63%)	3494473 (5.37%)	33600115 (42.45%)	31434807 (39.71%)
L5	85707326	70080879 (81.77%)	65899898 (94.03%)	4180981 (5.97%)	36079700 (42.10%)	34001179 (39.67%)
L7	72614352	59625107 (82.11%)	56228566 (94.30%)	3396541 (5.70%)	30705660 (42.29%)	28919447 (39.83%)
L8	89201344	72211452 (80.95%)	67737688 (93.80%)	4473764 (6.20%)	37246343 (41.76%)	34965109 (39.20%)

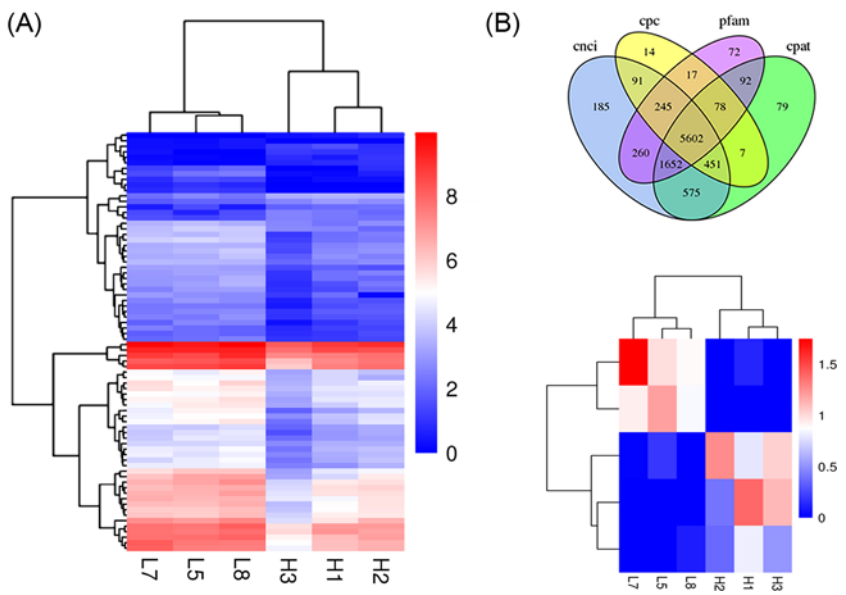

Figure 3. DE-mRNA and lncRNA

(**A**) Hierarchical cluster showing relative expression levels of 76 mRNAs between two groups; (**B**) non-coding transcripts identified by the four predictors were analyzed statistically, and then a Venn diagram of all predicted results was obtained. The lncRNA was predicted by four methods and 5602 lncRNA were found. The hierarchical clusters show the relative expression of five lncRNAs between two groups.

5′ and 3′ ends (Figure 2). These findings suggest that the sequencing data were highly reliable (Table 1). The mapping rate to the *O. aries* reference genome (Oar_v3.1) of our clean data was between 80.95 and 82.17% (Table 2).

Genome-wide identification of DE-mRNAs and DE-lncRNAs

For further analysis, 76 DE-mRNAs were identified between HP and LP Hu sheep (Figure 3A), 66 of which were up-regulated and 10 of which were down-regulated, with 4 identified as new genes in sheep (Supplementary Table S2). Based on the results of the comparison, 2424 new genes were discovered including 1529 functional annotations, by analyzing alternative splicing predictions, optimizing gene structure, and exploring new genes. Furthermore, 5602 lncRNAs were obtained using four prediction methods, and 5 were found to differ significantly between the two groups ($P<0.05$) (Figure 3B). The hierarchical clusters of the DE-mRNA and DE-lncRNA revealed the expression patterns in HP and LP ewes (Figure 3A,B).

© 2018 The Author(s). This is an open access article published by Portland Press Limited on behalf of the Biochemical Society and distributed under the Creative Commons Attribution License 4.0 (CC BY).

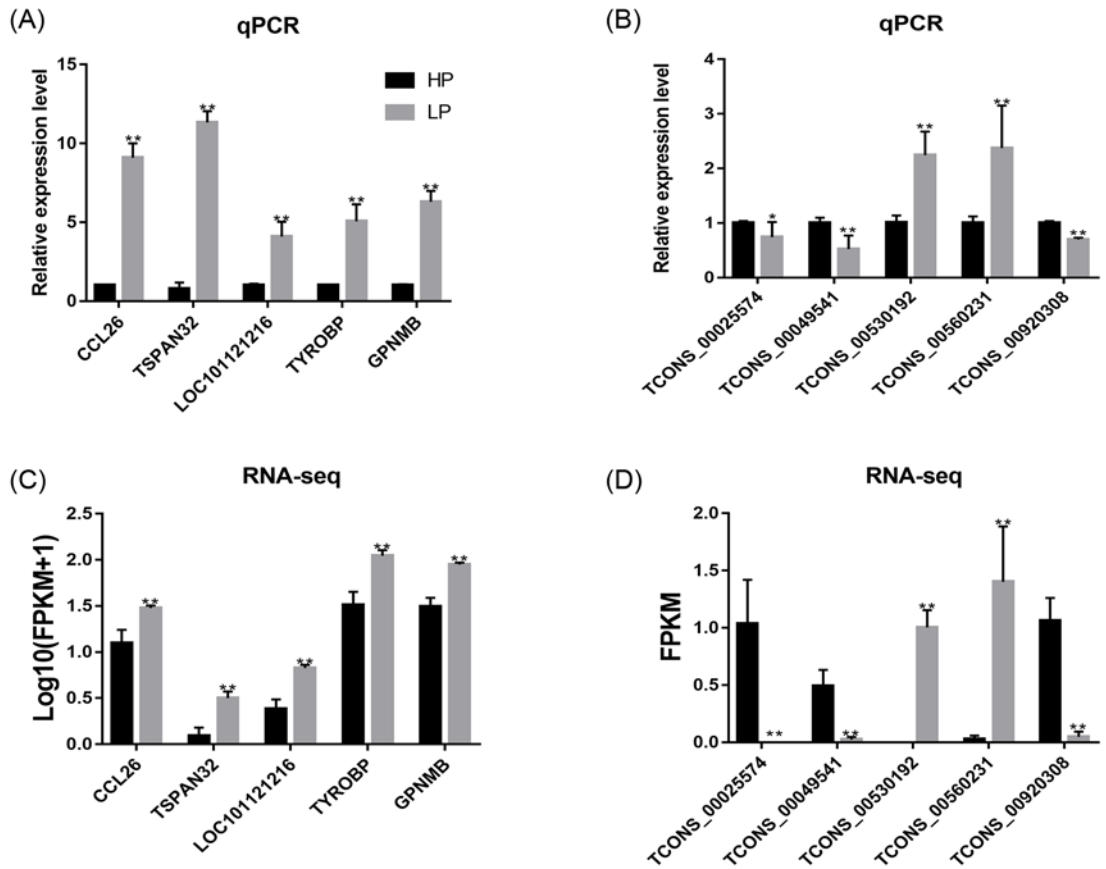

Figure 4. Validation of RNA-seq results using qRT-PCR and RNA-seq, respectively

(**A**,**B**) The relative expression of DE-mRNA and DE-lncRNA was determined by q-PCR. Comparisons by independent-sample *t* test, using SPSS 24.0. *: $P<0.05$; **: $P<0.01$. (**C**) RNA-seq data of DE-mRNA; relative expression level, normalized by $\log_{10}$ (FPKM + 1). (**D**) RNA-seq data of DE-lncRNA; relative expression level, normalized by FPKM. Abbreviations: CCL26, C–C motif chemokine ligand 26; *GPNMB*, glycoprotein nmb*; LOC101121216*, serum amyloid A protein-like; *TSPAN32*, tetraspanin 32; *TYROBP*, TYRO protein tyrosine kinase binding protein.

Validation of RNA-seq data by real-time PCR

To validate the RNA-seq data, we selected five DE-mRNAs and five DE-lncRNAs and determined the expression of these RNAs by real-time PCR (Figure 4). The expression of each mRNA or lncRNA was examined in the HP and LP groups, and the results were consistent with those obtained by sequencing. Primers of mRNA and lncRNA are shown in Supplementary Table S1.

Functional annotation and enrichment analysis

To further elucidate the functions of the DE-mRNAs and DE-lncRNAs, GO enrichment analysis was performed using topGO to search the most significant GO term of DE-mRNAs and the target genes of DE-lncRNAs. All of these were assigned to biological processes, cellular components, and molecular function, respectively. Moreover, organ morphogenesis, tissue development, immune system process, regulation of reproductive hormone biosynthetic process, and positive regulation of endothelial cell apoptotic process were identified as significantly enriched GO terms in DE-mRNAs (KS < 0.05, KS: *P*-value of Kolmogorov–Smirnov test, the smaller the KS value, the more significant the enrichment) (Supplementary Tables S3–S5). We also found that most DE-mRNAs were assigned to the GO terms of biological processes (Figure 5A). The targets of DE-lncRNAs were mostly enriched in immune system process, cell differentiation, and tissue development. The most enriched GO terms for DE-mRNAs and target genes in each comparison are shown in Figure 5A,C, respectively. According to the KEGG analysis, 60 (DE-mRNAs) and 6 (target gene of DE-lncRNAs) were assigned to 33 and 19 pathways, respectively. The most enriched pathway of DE-mRNA and

© 2018 The Author(s). This is an open access article published by Portland Press Limited on behalf of the Biochemical Society and distributed under the Creative Commons Attribution License 4.0 (CC BY).

Bioscience Reports (2018) **38** BSR20171350
https://doi.org/10.1042/BSR20171350

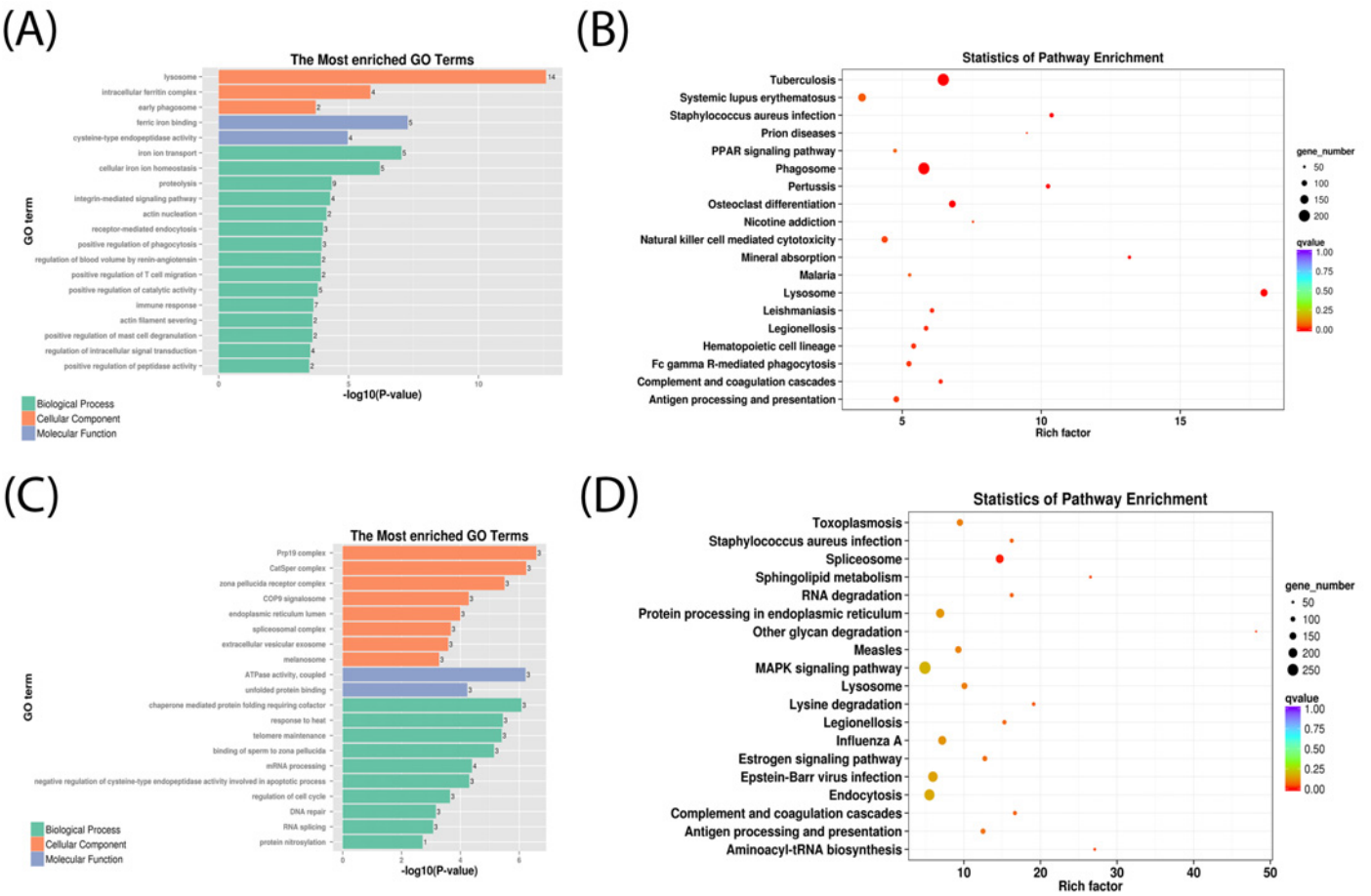

Figure 5. Top GO and KEGG pathway enrichment analyses of DE-mRNAs and target genes of DE-lncRNAs

(**A**) Top 20 GO terms of DE-mRNAs. (**B**) Top 20 pathways of DE-mRNAs. (**C**) Top 20 GO terms of the target genes of DE-lncRNAs. (**D**) Top 20 pathways of the target genes of DE-lncRNAs.

target genes of DE-lncRNA are shown in Figure 5B,D. They are predominantly associated with immune functions, such as phagosomes, lysosomes, and antigen processing and presentation, by DE-mRNAs ($P<0.05$).

Protein co-expression network and lncRNA–mRNA interaction network

To better illustrate the relationships between mRNAs and lncRNA, we constructed two co-expression networks (Figure 6A). Co-expression networks cluster multiple transcripts into functional modules based on the correlations with gene expression. We selected 48 DE-mRNAs to construct functional networks by referring to the STRING database, with each gene corresponding to a node. Two genes are connected by an edge, indicating a strong correlation (i.e. either positive or negative). Within the network analysis, we focussed on genes that interact with five more other genes; *C1qA*, *CD53*, cathepsin B (*CTSB*), *CTSS*, *TYROBP*, and *AIF1* were hub genes in the network. In order to understand the effect of lncRNA on the regulation of lnRNA, we constructed an mRNA–lncRNA regulatory network, which consisted of nodes, including 28 mRNAs and four lncRNAs (Figure 6B). These lncRNAs were predicted to regulate their targets by a *trans*-action mode.

Expression pattern of CTSB and CTSD in ovaries

In the present study, we found that most DE-mRNAs were enriched in the lysosome pathway. Two proteases, CTSB and CTSD, are involved in the function of lysosomes, and their genes are differentially expressed between HP ewes and LP ewes. Both the *CTSB* and *CTSD* genes are expressed in granulosa cells, and their expression are regulated by LH concentration [29]. The results obtained using peripheral blood from HP ewes revealed that the LH concentration was higher than that from LP ewes. Notably, the high LH concentration in HP ewes could reduce the expression of *CTSB*

© 2018 The Author(s). This is an open access article published by Portland Press Limited on behalf of the Biochemical Society and distributed under the Creative Commons Attribution License 4.0 (CC BY).

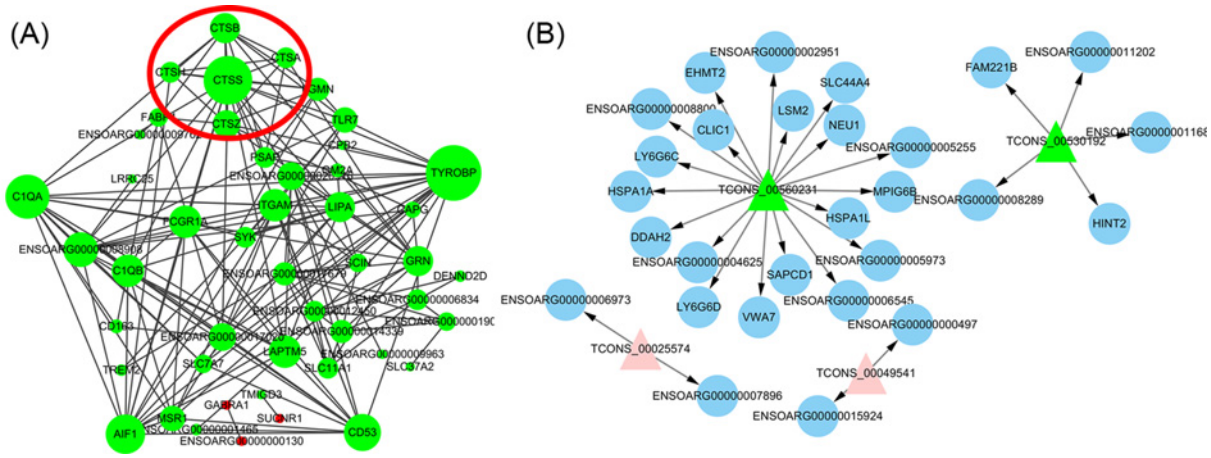

Figure 6. Network between DE-mRNAs and DE-lncRNAs

(**A**) Using STRING, the network of mRNA was constructed with 48 DE-mRNAs, and a significant interaction between these genes was found. Green nodes represent up-regulated genes, pink nodes represent down-regulated genes. The size of the node represents the number of genes that interact with it, the larger the node, the more genes that interact with it. Amongst the red circles is a member of the cathepsins family such as *CTSB*. (**B**) Four DE-lncRNAs were used to construct a network between lncRNA and mRNA. The nodes of the triangle represent lncRNA, and the circular nodes represent mRNA. Green nodes represent up-regulated genes, pink nodes represent down-regulated genes.

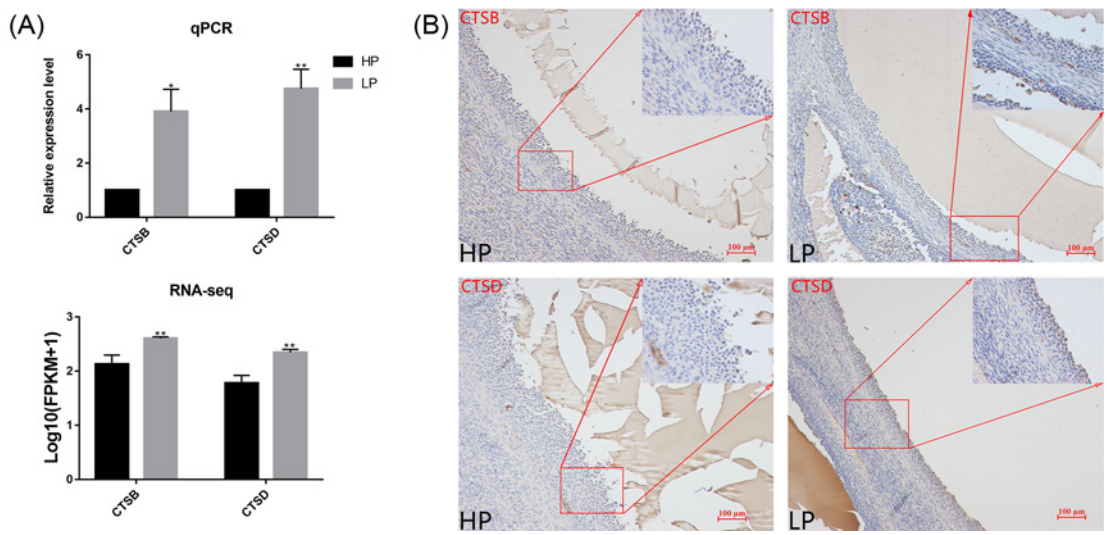

Figure 7. The pattern of *CTSB* and *CTSD* expression in the ovaries

(**A**) The relative expression level of *CTSB* and *CTSD* as determined by qRT-PCR, and the RNA-seq data of *CTSB*/*CTSD* relative expression, normalized by $\log_{10}$ (FPKM + 1). Comparisons were made using independent-sample *t* test, with SPSS 24.0. *: $P<0.05$; **: $P<0.01$. *CTSB* and *CTSD* primers are shown in Supplementary Table S1. (**B**) Representative immumohistochemical staining for *CTSB* and *CTSD* in the ovaries of HP and LP ewes. *CTSB* and *CTSD* proteins were both positively expressed in granulosa cells.

and *CTSD* in ovaries compared with that in LP ewes. Therefore, we hypothesized that CTSB and CTSD play very important roles in granulosa cells before ovulation, and may influence the litter size in ewes. In order to determine the expression pattern of *CTSB* and *CTSD* in sheep ovaries, we performed qRT-PCR and immumohistochemical staining. Similar to the results obtained with RNA-seq, the expression of *CTSB* and *CTSD* was significantly ($P<0.01$) higher in LP ewes than in HP ewes (Figure 7A). For immumohistochemical staining, we found that both *CTSB* and *CTSD* were expressed in the granulosa cells of mature follicles (>2.5 mm) of Hu sheep ovaries, as reported in other animals [30-32] (Figure 7B).

© 2018 The Author(s). This is an open access article published by Portland Press Limited on behalf of the Biochemical Society and distributed under the Creative Commons Attribution License 4.0 (CC BY).

Bioscience Reports (2018) **38** BSR20171350
https://doi.org/10.1042/BSR20171350

Discussion

Mammalian genomes encode thousands of lncRNAs. lncRNAs have gained widespread attention due to their roles in gene regulatory networks, and in a wide range of biological processes [33,34]. To date, many studies have associated the dysregulation of lncRNAs with reproduction, including germ cell formation, early embryo implantation and development, and reproductive hormone regulation. The present study examined the expression profile of mRNAs and lncRNAs in sheep ovaries associated with prolificacy, and found that mRNAs and lncRNAs were differentially expressed in the different groups analyzed. Further analyses of the interaction networks of mRNAs and lncRNA indicated that these DE-mRNA and lncRNA expression profiles might play key roles in sheep prolificacy.

The levels of E2, FSH, and LH are critical for follicle development and ovulation, and their effects on ovaries will ultimately affect litter size. The reproductive cycle of sheep usually includes three or four follicular waves, and the occurrence of follicular waves is largely controlled by dynamic changes in FSH levels, the diameter of a mature follicle affects the reactivity of the ewes to FSH. When sheep's reactivity to FSH is reduced, the number of follicular waves will reduce, resulting in low ovulation rates. [35]. E2 levels in the ewes were similar during the estrous cycle and in pre-ovulation, suggesting that ovarian regulation by E2 is not the main reason for the difference in litter size [36]. Thus, the E2 levels of two groups were measured during the estrous cycle and during pre-ovulation; however, the results revealed no significant differences between the two groups of ewes. FSH in synergy with LH stimulates follicle maturation and ovulation. FSH and LH play important roles in follicular development [37]. A high FSH/LH ratio during the early stage of follicular development promotes primordial follicle entry into the pre-antral follicle [38]. The lower the ratio of FSH/LH before ovulation, the greater the litter size [39]. However, in our present study, there were no significant differences in the plasma concentrations of E2 and FSH between the HP and LP groups, but the ratio of FSH/LH in HP ewes was significantly lower than that in LP ewes, which might result in higher litter size in the HP ewes. In addition, by amplifying the mutation sites in BMPR-1B, we found that the *FecB* genes of the eight experimental ewes were identical, and were all of the BB genotype. Therefore, in addition to the BB genotype mutation of BMPR-1B, other important factors may affect litter size in sheep.

In the present study, 76 DE-mRNAs and 5 DE-lncRNAs were identified by pairwise comparison. qRT-PCR analysis revealed that the results correlated well with the RNA-seq data. Using GO enrichment analysis, we identified some GO terms related to the immune response and inflammatory response, such as immune system process, antigen processing and presentation, and positive regulation of interleukin-1β secretion (Supplementary Table S3). These results may indicate that the immune-like response that occurs before ovulation, approaching the LH peak, might affect the litter size of Hu sheep. Additionally, some GO terms related to reproductive hormone metabolism were found in our study, including regulation of testosterone biosynthetic process, progesterone metabolic process, androsterone dehydrogenase (B-specific) activity, and dihydrotestosterone 17-β-dehydrogenase activity; both these hormones were affected by LH [40] (Supplementary Tables S3 and S5). Conversely, the GO terms lysosomal membrane and positive regulation of endothelial cell apoptotic process were associated with apoptosis of ovarian cells, including granulosa cells. Using KEGG pathway enrichment analysis, we were unable to identify the pathway directly associated with reproduction; however, the antigen processing and presentation, and natural killer cell mediated cytotoxicity pathways are involved in the immune response (Supplementary Table S8). GO and KEGG enrichment data indicated that genes involved in the immune response and those associated with lysosomes might play important roles in ovulation. Changes in the expression of *C1q*, *TLRs*, and *cathepsin* genes that associated with the immune response were also found in other investigators' studies of ovulation, it was similar to our study [41].

In recent years, ovulation has been described as a complex process involving an inflammatory and immune response, which includes follicular development, final follicle rupture, and the release of oocytes, followed by the formation of the corpus luteum [42-44]. Ovulation can up-regulate the expression of genes related to the apoptosis of follicular cells, and can then lead to physiological damage of the follicles. However, increased plasma LH concertation may counteract this damage through the differential expression of some mRNAs and lncRNAs between HP and LP ewes. Allograft inflammatory factor 1 (AIF-1) is involved in macrophage activation, and is constitutively expressed in monocytes and macrophages. Small populations of macrophages are found in the ovaries, and these are essential for tissue homeostasis and normal ovarian function. The number of macrophages varies depending on the stage of the ovarian cycle, but these cells are mostly associated with the corpus luteum and follicular atresia [45]. Macrophages resident in the Graafian follicles have great influence on ovulation and corpus luteum formation [46]. As a class of transmembrane recognition receptors, TLRs regulate the immune response by stimulating the release of cytokines during inflammation-like processes [47]. Up-regulation of TLR7 has been found in the ovaries of LP ewes, and in the membranes of intracellular endosomes and lysosomes, where it is involved in lysosomal function [48]. Furthermore, the pathway related to TLRs directly impacts granulosa cell function by controlling steroidogenesis and interacting

© 2018 The Author(s). This is an open access article published by Portland Press Limited on behalf of the Biochemical Society and distributed under the Creative Commons Attribution License 4.0 (CC BY).

with FSH signaling [49]. Moreover, *TLR* gene expression could be regulated by gonadotropins [50]. In the present study, cathepsin genes (*CTSA*, *CTSB*, *CTSD*, *CTSH*, *CTSS*, *CTSZ*) and other lysosome-related genes (*lipase A*, lysosomal acid type, *LIPA*; legumain, *LGMN*) were up-regulated in LP ewes. The cathepsin family includes proteolytic enzymes that break down many proteins and possess a broad range of proteolytic properties. This family of proteases is mainly found in lysosomes, cytoplasm, and endosomes [51]. To delineate the differential expression patterns, mouse cathepsins B, K, S, and Z were reported to be expressed in developing oocyte and granulosa cells [31]. The abundance of CTSB, S, K, and Z mRNA in cumulus cells may be related to oocyte quality [32], Therefore, we speculated that the higher expression of CTSB, S, and Z may be one explanation for the low prolificacy of LP ewes. CTSB and CTSD are two common cathepsins, which are involved in apoptosis. Both these proteins are regulated by LH [52]. CTSB is involved in the regulation of apoptosis during serum-starvation in follicles, which suggests that CTSB might play a regulatory role in follicular apoptosis [30]. Conversely, reactive oxygen species (ROS) is also a necessary signal for ovulation, which may be triggered by LH [53]. ROS are key signaling modules involved in the initiation of apoptosis in antral follicles, and granulosa cells of antral follicles [54]. LH surge increases ROS levels, which can lead to the release of lysosomal enzymes, such as CTSB and CTSD, subsequently triggering apoptosis [55,56].

Previous studies have shown that mRNAs and lncRNAs may be involved in ovarian function and follicular development, thus regulating the fecundity of female animals [57,58]. We constructed a network diagram of lncRNAs and mRNAs to determine the regulation of mRNA by lncRNA. We identified some target genes, such as heat shock protein family A (Hsp70) member 1 like (HSPA1L), Hsp70 member 1A (HSPA1A), and histidine triad nucleotide binding protein 2 (HINT2), which are involved in apoptosis. HSPA1L and HSPA1A are members of the HSP70 family, and the HSP70 family is involved in lysosomal stability [59]. Once the lysosomal structure is unstable, it will lead to protease leakage, and then to apoptosis [56]. HSPA1 can block apoptosis by inhibiting BAX activation. In addition, HSPA1 can interact directly with the mitochondrial pathway, which may also block apoptosis [21]. HSPA1L and HSPA1A are predicted to be target genes for lncRNA *TCONS_00560231*, suggesting that lncRNA *TCONS_00560231* may also be involved in the regulation of granulosa cell apoptosis. As a member of a superfamily of histidine triad hydrolases, *HINT2* has been found to affect mitochondria-dependent apoptosis in hepatocytes [60]. *HINT2* is expressed in the mitochondria of adrenal cortical cells and is involved in the steroidogenic response of calcium-dependent and calcium-independent agonists. Calcium-dependent actions of *HINT2* on steroidogenesis may be associated with their ability to maintain mitochondrial potential. Moreover, *HINT2* affects the basic metabolism of certain nucleotides, which may play an important role in the activation of protein kinases and the interaction with certain transcription factors in mitochondrial metabolism. Thus, *CTSD* and *CTSB* may activate mitochondria-dependent apoptosis in granulosa cells [56], having the same effect as lncRNA *TCONS_00530192* regulated *HINT2*. *TCONS_00530192* may be involved in granulocyte apoptosis by regulating *HINT2*.

Generally, we found that the BB-type mutation in BMPR-1B may represent only one factor limiting increased litter size. LH levels in HP ewes were significantly higher than those in LP ewes before ovulation. The difference in LH concentration in the peripheral blood during ovulation might result in the differential expression of mRNA and lncRNA in the ovaries of HP and LP ewes. Ovulation is considered to be an inflammatory response. In this process, some inflammation-related genes, such as *AIF1*, *TYROBP*, *SLC11A1*, and *PYCARD*, and some immune-related genes, such as *TLR7*, *CCL26*, *C1qA*, and *C1qB* are up-regulated. The high expression of these genes leads to increased expression of lysosomal-related genes, such as *CTSD* and *CTSB*, which may be closely related to apoptosis. *CTSS*, *CTSB*, and *CTSZ* are also regulated by LH and are used as markers to assess oocyte quality [32,61]. Moreover, some lncRNAs can regulate their target genes in these reactions. For example, *TCONS_00560231* and *TCONS_00530192* may participate in granulosa cell apoptosis by regulating the *HSPA1A*, *HSPA1L*, and *HIT2*.

In the present study, we compared the levels of reproductive hormones before ovulation and the BMPR-1B polymorphism between HP and LP Hu sheep. Importantly, we showed the differential mRNA and lncRNA expression profiles associated with sheep prolificacy and constructed interaction networks amongst lncRNAs and mRNAs. Our study lays a solid foundation that may aid in elucidating the regulatory mechanisms of mRNAs and lncRNAs in sheep.

Acknowledgements

We thank all members of the Jiangsu Livestock Embryo Engineering Laboratory for their helpful advice.

Funding

This work was supported by the National Science and Technology Support Program [grant number 2015BAD03B05-06]; and the Key Research and Development Program of Jiangsu Province [grant number BE2015362].

© 2018 The Author(s). This is an open access article published by Portland Press Limited on behalf of the Biochemical Society and distributed under the Creative Commons Attribution License 4.0 (CC BY).

Competing interests

The authors declare that there are no competing interests associated with the manuscript.

Author contribution

X.F. and G.Z. helped implementation of simultaneous estrus. F.L. and Z.W. helped to prepare experiments. X.F. and J.P. assisted with qRT-PCR validation. T.Z., H.Y., and C.R. assisted with immunohistochemistry and ELISA. Y.Z. and F.W. were involved in the design and co-ordination of the study, helped to draft the manuscript, and provided funding. All authors read and approved the final manuscript.

Abbreviations

BAX, BCL2-Associated X; BMP15, bone morphogenetic protein 15; BMPR-1B, bone morphogenetic protein receptor, type 1B; cnci, coding-non-coding index; cpat, coding-potential assessment tool; cpc, coding potential calculator; CTSB, cathepsin B; CTSD, cathepsin D; DE-lncRNA, differentially expressed lncRNA; DE-mRNA, differentially expressed mRNA; E2, estradiol; FDR, false discovery rate; FPKM, fragments per kilobase of exon per million fragments mapped; FSH, follicle-stimulating hormone; GO, gene ontology; HINT2, histidine triad nucleotide binding protein 2; HP, high prolificacy; HRP, horseradish peroxidase; HSPA1A, heat shock protein family A member 1A; HSPA1L, heat shock protein family A member 1 like; Hsp70, heat shock protein family A; KEGG, Kyoto Encyclopedia of Genes and Genomes; KS, *P*-value of Kolmogorov–Smirnov test; LH, luteinizing hormone; lincRNA, long intergennic non-coding RNA; lncRNA, long non-coding RNA; LP, low prolificacy; ncRNA, non-coding RNA; OD, optical density; pfam, protein families database; qRT-PCR, quantitative real-time PCR; ROS, reactive oxygen species; TLR, toll-like receptors.

References

1 Bodin, L., Di Pasquale, E., Fabre, S., Bontoux, M., Monget, P., Persani, L. et al. (2007) A novel mutation in the bone morphogenetic protein 15 gene causing defective protein secretion is associated with both increased ovulation rate and sterility in Lacaune sheep. *Endocrinology* **148**, 393–400, https://doi.org/10.1210/en.2006-0764

2 Henry, D.G. (2005) Major genes affecting ovulation rate in sheep. *Genet. Select. Evol.* **37** (Suppl. 11), S11, https://doi.org/10.1186/1297-9686-37-S1-S11

3 Wang, W., Liu, S., Li, F.Y., Pan, X., Li, C., Zhang, X. et al. (2015) Polymorphisms of the ovine BMPR-IB, BMP-15 and FSHR and their associations with litter size in two Chinese indigenous sheep breeds. *Int. J. Mol. Sci.* **16**, 11385–11397, https://doi.org/10.3390/ijms160511385

4 Paz, E., Quinones, J., Bravo, S., Montaldo, H.H. and Sepulveda, N. (2015) Genotyping of BMPR1B, BMP15 and GDF9 genes in Chilean sheep breeds and association with prolificacy. *Anim. Genet.* **46**, 98–99, https://doi.org/10.1111/age.12254

5 Chu, M.X., Sang, L., Wang, J.Y., Fang, L. and Ye, S.C. (2005) Study on BMP15 and GDF9 as candidate genes for prolificacy of Small Tail Han sheep. *Acta Genet. Sin.* **32**, 38–45

6 Spizzo, R., Almeida, M.I., Colombatti, A. and Calin, G.A. (2012) Long non-coding RNAs and cancer: a new frontier of translational research? *Oncogene* **31**, 4577–4587, https://doi.org/10.1038/onc.2011.621

7 Zhao, X.Y. and Lin, J.D (2015) Long noncoding RNAs: a new regulatory code in metabolic control. *Trends Biochem. Sci.* **40**, 586–596, https://doi.org/10.1016/j.tibs.2015.08.002

8 Mattick, J.S. (2011) The central role of RNA in human development and cognition. *FEBS Lett.* **585**, 1600, https://doi.org/10.1016/j.febslet.2011.05.001

9 Sha, H., Liu, S. and Hao, Z. (2011) The sequence, structure and evolutionary features of HOTAIR in mammals. *BMC Evol. Biol.* **11**, 1–14

10 Mchugh, C.A., Chen, C.K., Chow, A., Surka, C.F., Tran, C., Mcdonel, P. et al. (2015) The Xist lncRNA interacts directly with SHARP to silence transcription through HDAC3. *Nature* **521**, 232, https://doi.org/10.1038/nature14443

11 Nagano, T. and Fraser, P. (2011) No-nonsense functions for long noncoding RNAs. *Cell* **145**, 178, https://doi.org/10.1016/j.cell.2011.03.014

12 Taylor, D.H., Chu, E.T., Spektor, R. and Soloway, P.D. (2015) Long non-coding RNA regulation of reproduction and development. *Mol. Reprod. Dev.* **82**, 932–956, https://doi.org/10.1002/mrd.22581

13 Li, J., Cao, Y., Xu, X., Xiang, H., Zhang, Z., Chen, B. et al. (2015) Increased new lncRNA-mRNA gene pair levels in human cumulus cells correlate with oocyte maturation and embryo development. *Reprod. Sci.* **22**, https://doi.org/10.1177/1933719115570911

14 Williams, J.M., Ball, M., Ward, A. and Moore, T. (2015) Psg22 expression in mouse trophoblast giant cells is associated with gene inversion and co-expression of antisense long non-coding RNAs. *Reproduction* **149**, 125, https://doi.org/10.1530/REP-14-0390

15 Macaulay, A.D., Gilbert, I., Caballero, J., Barreto, R., Fournier, E., Tossou, P. et al. (2014) The gametic synapse: RNA transfer to the bovine oocyte. *Biol. Reprod.* **91**, 90, https://doi.org/10.1095/biolreprod.114.119867

16 Cossetti, C., Lugini, L., Astrologo, L., Saggio, I., Fais, S. and Spadafora, C. (2014) Soma-to-germline transmission of RNA in mice xenografted with human tumour cells: possible transport by exosomes. *PLoS ONE* **9**, e101629, https://doi.org/10.1371/journal.pone.0101629

17 Pefanis, E., Wang, J., Rothschild, G., Lim, J., Kazadi, D., Sun, J. et al. (2015) RNA exosome regulated long non-coding RNA transcription controls super-enhancer activity. *Cell* **161**, 774–789, https://doi.org/10.1016/j.cell.2015.04.034

18 Gezer, U., Özgür, E., Cetinkaya, M., Isin, M. and Dalay, N. (2014) Long non-coding RNAs with low expression levels in cells are enriched in secreted exosomes. *Cell Biol. Int.* **38**, 1076–1079

© 2018 The Author(s). This is an open access article published by Portland Press Limited on behalf of the Biochemical Society and distributed under the Creative Commons Attribution License 4.0 (CC BY).

19 Nakagawa, S., Shimada, M., Yanaka, K., Mito, M., Arai, T., Takahashi, E. et al. (2014) The lncRNA Neat1 is required for corpus luteum formation and the establishment of pregnancy in a subpopulation of mice. *Development* **141**, 4618–4627, https://doi.org/10.1242/dev.110544
20 Miao, X., Luo, Q., Zhao, H. and Qin, X. (2016) Ovarian transcriptomic study reveals the differential regulation of miRNAs and lncRNAs related to fecundity in different sheep. *Sci. Rep.* **6**, 35299, https://doi.org/10.1038/srep35299
21 Kennedy, D., Jager, R., Mosser, D.D. and Samali, A. (2014) Regulation of apoptosis by heat shock proteins. *IUBMB Life* **66**, 327–338, https://doi.org/10.1002/iub.1274
22 Kong, L., Zhang, Y., Ye, Z.Q., Liu, X.Q., Zhao, S.Q., Wei, L. et al. (2007) CPC: assess the protein-coding potential of transcripts using sequence features and support vector machine. *Nucleic Acids Res.* **35**, W345, https://doi.org/10.1093/nar/gkm391
23 Sun, L., Luo, H., Bu, D., Zhao, G., Yu, K., Zhang, C. et al. (2013) Utilizing sequence intrinsic composition to classify protein-coding and long non-coding transcripts. *Nucleic Acids Res.* **41**, e166, https://doi.org/10.1093/nar/gkt646
24 Liguo Wang, H.J.P., Dasari, S., Wang, S., Kocher, J.-P. and Li, W, (2013) CPAT: Coding-Potential Assessment Tool using an alignment-free logistic regression model. *Nucleic Acids Res.* **41**, e74, https://doi.org/10.1093/nar/gkt006
25 Finn, R.D., Bateman, A., Clements, J., Coggill, P., Eberhardt, R.Y., Eddy, S.R. et al. (2014) Pfam: the protein families database. *Nucleic Acids Res.* **42**, D222, https://doi.org/10.1093/nar/gkt1223
26 Trapnell, C., Williams, B.A., Pertea, G., Mortazavi, A., Kwan, G., van Baren, M.J. et al. (2010) Transcript assembly and quantification by RNA-Seq reveals unannotated transcripts and isoform switching during cell differentiation. *Nat. Biotechnol.* **28**, 511–515, https://doi.org/10.1038/nbt.1621
27 Li, J., Ma, W., Zeng, P., Wang, J., Geng, B., Yang, J. et al. (2015) LncTar: a tool for predicting the RNA targets of long noncoding RNAs. *Brief. Bioinformatics* **16**, 806–812, https://doi.org/10.1093/bib/bbu048
28 Mao, X., Cai, T., Olyarchuk, J.G. and Wei, L. (2005) Automated genome annotation and pathway identification using the KEGG Orthology (KO) as a controlled vocabulary. *Bioinformatics* **21**, 3787–3793, https://doi.org/10.1093/bioinformatics/bti430
29 McRae, R.S., Johnston, H.M., Mihm, M. and O'Shaughnessy, P.J. (2005) Changes in mouse granulosa cell gene expression during early luteinization. *Endocrinology* **146**, 309–317, https://doi.org/10.1210/en.2004-0999
30 Eykelbosh, A.J. and Van Der Kraak, G. (2010) A role for the lysosomal protease cathepsin B in zebrafish follicular apoptosis. *Comp. Biochem. Physiol. A Mol. Integr. Physiol.* **156**, 218–223, https://doi.org/10.1016/j.cbpa.2010.02.005
31 Jokimaa, V., Oksjoki, S., Kujari, H., Vuorio, E. and Anttila, L. (2001) Expression patterns of cathepsins B, H, K, L and S in the human endometrium. *Mol. Hum. Reprod.* **7**, 73, https://doi.org/10.1093/molehr/7.1.73
32 Bettegowda, A., Patel, O.V., Lee, K.B., Park, K.E., Salem, M., Yao, J. et al. (2008) Identification of novel bovine cumulus cell molecular markers predictive of oocyte competence: functional and diagnostic implications. *Biol. Reprod.* **79**, 301, https://doi.org/10.1095/biolreprod.107.067223
33 Men, Y., Fan, Y., Shen, Y., Lu, L. and Kallen, A.N. (2016) The steroidogenic acute regulatory protein (StAR) is regulated by the H19/let-7 axis. *Endocrinology*, https://doi.org/10.1210/en.2016-1340
34 Kornienko, A.E., Dotter, C.P., Guenzl, P.M., Gisslinger, H., Gisslinger, B., Cleary, C. et al. (2016) Long non-coding RNAs display higher natural expression variation than protein-coding genes in healthy humans. *Genome Biol.* **17**, 14, https://doi.org/10.1186/s13059-016-0873-8
35 Bartlewski, P.M., Baby, T.E. and Giffin, J.L. (2011) Reproductive cycles in sheep. *Anim. Reprod. Sci.* **124**, 259–268, https://doi.org/10.1016/j.anireprosci.2011.02.024
36 Oliveira, M.F., D'Amato, C., Barros, F., Perini, A., Lima, M., Oliveira, L. et al. (2012) Influence of season on super-ovulatory response and embryo yield of Santa Ines ewes submitted to FSH treatment started near the time of emergence of the last follicular wave. *Reprod. Domest. Anim.* **47**, 83–84
37 Portela, A.M.L.R., Ribeiro, R.P., Costa, J.J.N., Rossi, R.O.D.S., Passos, J.R.S., Vasconcelos, G.L. et al. (2014) Effects of different concentrations of concanavalin A and follicle stimulating hormone on goat primordial follicles activation, survival and gene expression. *Small Rumin. Res.* **116**, 183–191, https://doi.org/10.1016/j.smallrumres.2013.10.021
38 Boscos, C.M., Samartzi, F.C., Dellis, S., Rogge, A., Stefanakis, A. and Krambovitis, E. (2002) Use of progestagen-gonadotrophin treatments in estrus synchronization of sheep. *Theriogenology* **58**, 1261–1272, https://doi.org/10.1016/S0093-691X(02)01040-3
39 D'Alessandro, A.G., Martemucci, G. and Taibi, L. (2005) How the FSH/LH ratio and dose numbers in the p-FSH administration treatment regimen, and insemination schedule affect superovulatory response in ewes. *Theriogenology* **63**, 1764–1774, https://doi.org/10.1016/j.theriogenology.2004.08.002
40 Gungor, O., Cenesz, M., Pancarc, S.M., Yldz, S., Kaya, M., Kacar, C. et al. (2007) Effects of different intravaginal progesterone releasing devices on estrous synchronization and LH surge in fat-tailed ewes during non-breeding season. *Med. Weter.* **63**, 1316–1319
41 Richards, J.S., Liu, Z. and Shimada, M. (2008) Immune-like mechanisms in ovulation. *Trends Endocrinol. Metab.* **19**, 191–196, https://doi.org/10.1016/j.tem.2008.03.001
42 Espey, L.L. (1980) Ovulation as an inflammatory reaction—a hypothesis. *Biol. Reprod.* **22**, 73–106, https://doi.org/10.1095/biolreprod22.1.73
43 Richards, J.S., Russell, D.L., Ochsner, S.A. and Espey, L.L. (2003) Ovulation: new dimensions and new regulators of the inflammatory-like response. *Annu. Rev. Physiol.* **64**, 69–92, https://doi.org/10.1146/annurev.physiol.64.081501.131029
44 Boots, C.E. and Jungheim, E.S. (2015) Inflammation and human ovarian follicular dynamics. *Semin. Reprod. Med.* **33**, 270, https://doi.org/10.1055/s-0035-1554928
45 Sheldon, I.M. and Bromfield, J.J. (2011) Innate immunity in the human endometrium and ovary. *Am. J. Reprod. Immunol.* **66**, 63–71, https://doi.org/10.1111/j.1600-0897.2011.01034.x
46 Wu, R., Kh, V.D.H., Ryan, N.K., Norman, R.J. and Robker, R.L. (2004) Macrophage contributions to ovarian function. *Hum. Reprod. Update* **10**, 119, https://doi.org/10.1093/humupd/dmh011
47 Iwasaki, A. and Medzhitov, R. (2010) Regulation of adaptive immunity by the innate immune system. *Science* **327**, 291–295, https://doi.org/10.1126/science.1183021
48 Lester, S.N. and Li, K. (2014) Toll-like receptors in antiviral innate immunity. *J. Mol. Biol.* **426**, 1246–1264, https://doi.org/10.1016/j.jmb.2013.11.024

© 2018 The Author(s). This is an open access article published by Portland Press Limited on behalf of the Biochemical Society and distributed under the Creative Commons Attribution License 4.0 (CC BY).

49 Shan, H., Williams, E.J., Lilly, S.T., Gilbert, R.O., Dobson, H., Bryant, C.E. et al. (2007) Ovarian follicular cells have innate immune capabilities that modulate their endocrine function. *Reproduction* **134**, 683, https://doi.org/10.1530/REP-07-0229
50 Woods, D.C., Schorey, J.S. and Johnson, A.L. (2009) Toll-like receptor signaling in hen ovarian granulosa cells is dependent on stage of follicle maturation. *Reproduction* **137**, 987–996, https://doi.org/10.1530/REP-08-0320
51 Cheng, X.W., Huang, Z., Kuzuya, M., Okumura, K. and Murohara, T. (2011) Cysteine protease cathepsins in atherosclerosis-based vascular disease and its complications. *Hypertension* **58**, 978–986, https://doi.org/10.1161/HYPERTENSIONAHA.111.180935
52 Reference deleted
53 Shkolnik, K., Tadmor, A., Ben-Dor, S., Nevo, N., Galiani, D. and Dekel, N. (2011) Reactive oxygen species are indispensable in ovulation. *Proc. Natl. Acad. Sci. U.S.A.* **108**, 1462, https://doi.org/10.1073/pnas.1017213108
54 Devine, P.J., Perreault, S.D. and Luderer, U. (2012) Roles of reactive oxygen species and antioxidants in ovarian toxicity. *Biol. Reprod.* **86**, 27, https://doi.org/10.1095/biolreprod.111.095224
55 Zhao, M., Antunes, F., Eaton, J.W. and Brunk, U.T. (2003) Lysosomal enzymes promote mitochondrial oxidant production, cytochrome c release and apoptosis. *Eur. J. Biochem.* **270**, 3778–3786, https://doi.org/10.1046/j.1432-1033.2003.03765.x
56 Aits, S. and Jaattela, M. (2013) Lysosomal cell death at a glance. *J. Cell Sci.* **126**, 1905–1912, https://doi.org/10.1242/jcs.091181
57 Gao, Q., Ren, H., Chen, M., Niu, Z., Tao, H., Jia, Y. et al. (2016) Long non-coding RNAs regulate effects of β-crystallin B2 on mouse ovary development. *Mol. Med. Rep.* **14**, 4223–4231, https://doi.org/10.3892/mmr.2016.5761
58 Bakhtiarizadeh, M.R., Hosseinpour, B., Arefnezhad, B., Shamabadi, N. and Salami, S.A. (2016) *In silico* prediction of long intergenic non-coding RNAs in sheep. *Genome* **59**, 263, https://doi.org/10.1139/gen-2015-0141
59 Yamashima, T. (2012) Hsp70.1 and related lysosomal factors for necrotic neuronal death. *J. Neurochem.* **120**, 477–494, https://doi.org/10.1111/j.1471-4159.2011.07596.x
60 Martin, J., Magnino, F., Schmidt, K., Piguet, A.C., Lee, J.S., Semela, D. et al. (2006) Hint2, a mitochondrial apoptotic sensitizer down-regulated in hepatocellular carcinoma. *Gastroenterology* **130**, 2179–2188, https://doi.org/10.1053/j.gastro.2006.03.024
61 Ashry, M., Lee, K.B., Mondal, M., Datta, T.K., Folger, J.K., Rajput, S.K. et al. (2015) Expression of TGFβ superfamily components and other markers of oocyte quality in oocytes selected by brilliant cresyl blue staining: relevance to early embryonic development. *Mol. Reprod. Dev.* **82**, 251, https://doi.org/10.1002/mrd.22468

© 2018 The Author(s). This is an open access article published by Portland Press Limited on behalf of the Biochemical Society and distributed under the Creative Commons Attribution License 4.0 (CC BY).

Supplementary Materials:Genome-wide differential expression profiling of mRNAs and lncRNAs associated with prolificacy in Hu sheep

Xu Feng, Fengzhe Li, Feng Wang, Guomin Zhang, Jing Pang, Caifang Ren,Tingting Zhang, Hua Yang, Ziyu Wang, Yanli Zhang

Table S1. Details of primer sequences, expected product sizes and Genbank accession numbers of genes used for qRT-PCR

Gene	Primer sequence(5′- 3′)	Product size(bp)	Accession number
CCL26	F:GATGTGGCCAAGTTCTGCTG R: TCGGCTGGGCACATACTTTC	148	XM_004020976.3
TSPAN32	F:AAGAAGTGGGTGTGGGCTTT R:CCTGGCCCAATTTGAAGGAC	144	NM_001114667.1
LOC101121216	F:GCCAACTACAAGGGTGCAGA R: TTGTTAGGCAGGCCAGCAG	257	XM_004019478.3
TYROBP	F:ATGCAACTGCTCCTCGTTGA R:GTGATGTGCTGTTTCCGGGT	159	XM_012120538.1
GPNMB	F:CCTGGTATTCCCCAGATGCC R:GTCCACGCTGTCCAGTTGTA	120	XM_004007790.3
TCONS_00025574	F:TGTCCGCTGCTGCCACTTCTA R: TAACGGGCTCCTGCTGGATGAG	132	--
TCONC_00049541	F:TGCTCAGAGGCTCAGTCGTGTT R: CCTCCCAGGCAGTTCAGTGGTA	194	--
TCONC_00530192	F:TGAAGCAGCAGAGGACACAGGT R:AGGTTGCTCAGTGGGTCAGAGG	113	--
TCONS_00560231	F:TGTTGCTGAAGTGGCAGGAACC R:TGTTGCTGAAGTGGCAGGAACC	232	--
TCONC_00920308	F:ACAAGGGAGGCTTGTTGGTG R: CTGAGTCCACTGCTTGGTGA	107	--
BMPR1B	F: GTGCCGTGAACGCACTAACA R: AGACAAAAACGTGCTCCTTCAA	559	NW_011942424.1
CTSB	F: TAGGCTGGGGAGTGGAGAAC R: AGTACTGATGAGTGCACGGC	159	NM_001308587.1
CTSD	F: GCCAGGACCCTGTGTCG R: GCACGTTGTTGACGGAGATG	174	XM_012171958.2
GAPDH	F:GTCAAGGCAGAGAACGGGAA R:GGTTCACGCCCATCACAAAC	232	XM_012166462.1

Table S2 The annotation of all DE-mRNAs

#ID	H1	H2	H3	L5	L7	L8	KEGG_annotation	Swissprot_annotation	nr_annotation
ENSOARG00000000130	4.124731689	3.726211631	4.766965461	1.500059367	1.97862319	2.079188317	K04809 |0|oas:101113104 |neuronal acetylcholine receptor subunit alpha-7-like; K04809 nicotinic acetylcholine receptor alpha-7 (A)	Neuronal acetylcholine receptor subunit alpha-7 (Precursor) GN=CHRNA7 OS=Bos taurus (Bovine) PE=2 SV=1	PREDICTED: LOW QUALITY PROTEIN: neuronal acetylcholine receptor subunit alpha-7-like [Ovis aries]
ENSOARG00000001465	3.405431396	0.137444089	1.201888662	5.810695249	7.093629207	5.51918253	--	GTPase IMAP family member 6 GN=GIMAP6 OS=Bos taurus (Bovine) PE=2 SV=1	PREDICTED: GTPase IMAP family member 7-like isoform 1 [Ovis aries]
ENSOARG00000001744	3.690314283	4.312226564	1.386111821	17.41025928	15.29002115	15.02386315	K14378 |7.4877e-159 |oas:101105447 |TREM2; triggering receptor expressed on myeloid cells 2; K14378 triggering receptor expressed on myeloid cells 2 (A)	Triggering receptor expressed on myeloid cells 1 (Precursor) GN=TREM1 OS=Bos taurus (Bovine) PE=2 SV=1	PREDICTED: triggering receptor expressed on myeloid cells 2 [Ovis aries]
ENSOARG00000001747	9.608946717	9.544950266	5.533109208	16.55068317	16.45007458	18.56610513	K01565 |0|oas:101121184 |SGSH; N-sulfoglucosamine sulfohydrolase; K01565 N-sulfoglucosamine sulfohydrolase [EC:3.10.1.1] (A)	Arylsulfatase A (Precursor) GN=ARSA OS=Bos taurus (Bovine) PE=2 SV=1	PREDICTED: N-sulphoglucosamine sulphohydrolase [Ovis aries]
ENSOARG00000002094	45.09405569	48.17747161	21.06712828	88.12350641	87.17829626	115.1314801	K12387 |1.27089e-176 |oas:101121575 |LAPTM5; lysosomal protein transmembrane 5; K12387 lysosomal-associated transmembrane protein (A)	Lysosomal-associated transmembrane protein 5 GN=LAPTM5 OS=Bos taurus (Bovine) PE=2 SV=1	PREDICTED: lysosomal-associated transmembrane protein 5 [Ovis aries]
ENSOARG00000002862	21.38892612	22.11104804	11.247039	35.56509038	46.84036821	41.66991902	K06545 |0|oas:443147 |EM4e; EM4e protein; K06545 CD163 antigen (A)	Soluble CD163 {ECO:0000250 |UniProtKB:Q86VB7} (Precursor) OS=Bos taurus (Bovine) PE=1 SV=2	PREDICTED: LOW QUALITY PROTEIN: uncharacterized protein LOC443147 [Ovis aries]
ENSOARG00000003347	0	0.865299456	0	2.120700616	1.417745551	3.22899783	K17359 |4.66952e-91 |oas:101120369 |TSPAN32; tetraspanin 32; K17359 tetraspanin-32 (A)	Parotid hormone (Precursor) OS=Sus scrofa (Pig) PE=1 SV=2	PREDICTED: tetraspanin-32 isoform X1 [Bos taurus]
ENSOARG00000003740	10.0528254	9.920952958	9.304096155	5.264629692	3.504580739	3.852621678	K10042 |0|oas:101122570 |SUCNR1; succinate receptor 1; K10042 succinate receptor 1 (A)	P2Y purinoceptor 1 GN=P2RY1 OS=Bos taurus (Bovine) PE=2 SV=1	PREDICTED: LOW QUALITY PROTEIN: succinate receptor 1 [Ovis aries]
ENSOARG00000003938	74.48804639	90.10096074	30.34384521	195.4406731	286.9303514	188.9630827	K01379 |7.61178e-64 |phd:102343491 |CTSD; cathepsin D; K01379 cathepsin D [EC:3.4.23.5] (A)	Cathepsin D (Precursor; Fragment) GN=CTSD OS=Ovis aries (Sheep) PE=1 SV=1	PREDICTED: cathepsin D [Pantholops hodgsonii]
ENSOARG00000004979	73.23556584	91.68820654	25.30948343	177.6899318	263.0103423	175.7671455	K01379 |3.70961e-65 |lve:103083086 |CTSD; cathepsin D; K01379 cathepsin D [EC:3.4.23.5] (A)	Cathepsin D (Precursor) GN=CTSD OS=Bos taurus (Bovine) PE=1 SV=2	Cathepsin D, partial [Bos mutus]
ENSOARG00000005167	40.58853255	47.26120421	16.01741606	102.4354699	89.21230915	144.5300588	K07992 |1.50732e-60 |chx:102175151 |TYROBP; TYRO protein tyrosine kinase binding protein; K07992 TYRO protein tyrosine kinase binding protein (A)	TYRO protein tyrosine kinase-binding protein (Precursor) GN=TYROBP OS=Bos taurus (Bovine) PE=3 SV=1	PREDICTED: TYRO protein tyrosine kinase-binding protein isoform X1 [Capra hircus]
ENSOARG00000005236	2.477200372	2.587320056	1.042626099	5.236503019	4.102433766	5.57565066	--	--	PREDICTED: V-set and immunoglobulin domain-containing protein 4-like [Balaenoptera acutorostrata scammoni]
ENSOARG00000006056	0.350541292	0.735692721	0.267072791	0.013869667	0.016362788	0.013772661	K04275 |0|phd:102330620 |LPAR4; lysophosphatidic acid receptor 4; K04275 lysophosphatidic acid receptor 4 (A)	Lysophosphatidic acid receptor 5 GN=LPAR5 OS=Bos taurus (Bovine) PE=2 SV=1	PREDICTED: lysophosphatidic acid receptor 4 isoform 1 [Ovis aries]
ENSOARG00000006715	7.029778122	5.851012315	5.239421294	2.885946587	2.434205337	3.053241637	--	Lysophosphatidic acid phosphatase type 6 (Precursor) GN=ACP6 OS=Bos taurus (Bovine) PE=1 SV=1	PREDICTED: acid phosphatase-like protein 2 [Ovis aries]
ENSOARG00000006834	17.24101709	12.50626968	8.129105924	23.02542106	28.31086641	36.89479204	K13625 |4.45307e-125 |phd:102335976 |ferritin light chain-like; K13625 ferritin light chain (A)	Ferritin light chain GN=FTL OS=Bos taurus (Bovine) PE=2 SV=3	ferritin light chain [Bos taurus]
ENSOARG00000006957	450.7029253	528.9135898	285.9054364	708.5575711	878.7012692	994.7942317	K12382 |0|oas:100135695 |PSAP; prosaposin; K12382 saposin (A)	Saposin-D (Precursor) GN=PSAP OS=Bos taurus (Bovine) PE=1 SV=3	PREDICTED: proactivator polypeptide isoform 1 [Ovis aries]
ENSOARG00000006985	38.36290587	41.61754012	16.30831894	61.93929705	66.19518534	79.3853893	K13289 |0|oas:101113615 |CTSA; cathepsin A; K13289 cathepsin A (carboxypeptidase C) [EC:3.4.16.5] (A)	Lysosomal protective protein 20 kDa chain (Precursor) GN=CTSA OS=Bos taurus (Bovine) PE=2 SV=1	PREDICTED: lysosomal protective protein [Ovis aries]
ENSOARG00000007110	7.194076423	10.87501055	2.799143814	35.21636177	23.71065745	35.23451252	K06560 |0|oas:101111081 |PLA2R1; phospholipase A2 receptor 1, 180kDa; K06560 mannose receptor, C type (A)	Soluble secretory phospholipase A2 receptor (Precursor) GN=PLA2R1 OS=Bos taurus (Bovine) PE=1 SV=1	PREDICTED: secretory phospholipase A2 receptor [Ovis aries]
ENSOARG00000007578	17.12478751	40.81953231	8.509724162	104.7540632	68.67295068	112.3830013	K05768 |0|oas:101123369 |SCIN; scinderin; K05768 gelsolin (A)	Adseverin GN=SCIN OS=Bos taurus (Bovine) PE=1 SV=1	PREDICTED: adseverin [Ovis aries]
ENSOARG00000007804	14.83490689	23.44150165	8.486058825	40.56778366	27.82037848	43.29150053	K01300 |0|oas:101112329 |CPB2; carboxypeptidase B2 (plasma); K01300 carboxypeptidase B2 [EC:3.4.17.20] (A)	Carboxypeptidase B2 (Precursor) GN=CPB2 OS=Bos taurus (Bovine) PE=1 SV=1	PREDICTED: carboxypeptidase B2 [Ovis aries]
ENSOARG00000007814	4.868073336	5.866350189	1.840311242	10.53162028	9.207296116	10.0162103	K05855 |0|oas:101105303 |SYK; spleen tyrosine kinase; K05855 spleen tyrosine kinase [EC:2.7.10.2] (A)	40 kDa tyrosine-protein kinase SYK GN=SYK OS=Sus scrofa (Pig) PE=1 SV=1	Tyrosine-protein kinase SYK, partial [Bos mutus]
ENSOARG00000007932	21.54335293	22.47508683	7.752600196	37.24691933	35.42141401	47.80070975	K18617 |8.1491e-89 |oas:101121889 |AIF1; allograft inflammatory factor 1; K18617 allograft inflammatory factor 1 (A)	Allograft inflammatory factor 1 GN=AIF1 OS=Bos taurus (Bovine) PE=2 SV=1	PREDICTED: allograft inflammatory factor 1 isoform 1 [Ovis aries]
ENSOARG00000007977	31.62425809	45.50613674	11.7525908	74.229938	76.03323158	92.45617357	K03987 |8.09548e-111 |oas:101123189 |C1QB; complement component 1, q subcomponent, B chain; K03987 complement C1q subcomponent subunit B (A)	Complement C1q subcomponent subunit B (Precursor) GN=C1QB OS=Bos taurus (Bovine) PE=1 SV=1	PREDICTED: complement C1q subcomponent subunit B [Ovis aries]
ENSOARG00000008001	10.74326797	12.32094882	3.815880836	21.7962624	23.5936009	28.62988712	K03986 |6.57665e-139 |oas:101102126 |C1QA; complement component 1, q subcomponent, A chain; K03986 complement C1q subcomponent subunit A (A)	Complement C1q subcomponent subunit A (Precursor) GN=C1QA OS=Bos taurus (Bovine) PE=2 SV=1	PREDICTED: complement C1q subcomponent subunit A isoform 1 [Ovis aries]
ENSOARG00000008164	29.82969509	42.59278664	13.22338713	63.58154898	61.63919853	75.44062491	--	Antimicrobial peptide eNAP-1 (Fragment) OS=Equus caballus (Horse) PE=1 SV=1	PREDICTED: LOW QUALITY PROTEIN: granulins [Ovis aries]
ENSOARG00000008167	3.415994637	4.509894769	1.143103314	11.10103531	12.33110595	13.88661218	--	Leukocyte-specific transcript 1 protein GN=LST1 OS=Macaca mulatta (Rhesus macaque) PE=3 SV=1	PREDICTED: leukocyte-specific transcript 1 protein [Ovis aries]
ENSOARG00000008426	0.118828208	0.572024501	0.185908663	3.836512015	1.815296136	4.4616026	K00486 |0|oas:101121026 |KMO; kynurenine 3-monooxygenase (kynurenine 3-hydroxylase); K00486 kynurenine 3-monooxygenase [EC:1.14.13.9] (A)	Kynurenine 3-monooxygenase {ECO:0000255 |HAMAP-Rule:MF_03018} OS=Sus scrofa (Pig) PE=2 SV=2	PREDICTED: kynurenine 3-monooxygenase [Ovis aries]
ENSOARG00000008438	48.12028763	56.02308731	17.90598024	89.77885072	75.74290712	95.87426755	K12383 |1.29262e-113 |oas:101105496 |GM2A; GM2 ganglioside activator; K12383 ganglioside GM2 activator (A)	Ganglioside GM2 activator (Precursor) GN=GM2A OS=Macaca fascicularis (Crab-eating macaque) PE=2 SV=2	PREDICTED: ganglioside GM2 activator [Ovis aries]
ENSOARG00000008861	1.211966985	1.618350264	1.038459151	3.49164358	3.060693063	4.668159976	K16852 |0|oas:101120971 |SLAMF6; SLAM family member 6; K16852 SLAM family member 6 (A)	Signaling lymphocytic activation molecule (Precursor) GN=SLAMF1 OS=Canis familiaris (Dog) PE=1 SV=1	PREDICTED: SLAM family member 6 [Ovis aries]
ENSOARG00000008908	9.412649319	11.28054377	5.198960736	19.1647851	24.88969368	23.90837168	K12799 |2.51557e-141 |oas:101105208 |PYCARD; PYD and CARD domain containing; K12799 apoptosis-associated speck-like protein containing a CARD (A)	Apoptosis-associated speck-like protein containing a CARD GN=PYCARD OS=Bos taurus (Bovine) PE=2 SV=1	PREDICTED: apoptosis-associated speck-like protein containing a CARD isoform 1 [Ovis aries]
ENSOARG00000009000	7.269795274	9.389145972	3.013467114	13.9672554	15.26033789	18.62940135	K06461 |0|oas:443217 |ITGAM, C3bi, CD11B, CR3; integrin, alpha M (complement component 3 receptor 3 subunit); K06461 integrin alpha M (A)	Integrin alpha-L (Precursor) GN=ITGAL OS=Bos taurus (Bovine) PE=2 SV=1	integrin alpha-M precursor [Ovis aries]
ENSOARG00000009344	5.187703978	3.201801568	5.530540123	15.56334897	11.62343637	14.24237942	K08753 |2.75008e-91 |oas:100137067 |FABP4; fatty acid binding protein 4, adipocyte; K08753 fatty acid-binding protein 4, adipocyte (A)	Fatty acid-binding protein, adipocyte GN=FABP4 OS=Cervus elaphus (Red deer) PE=2 SV=1	fatty acid-binding protein, adipocyte [Ovis aries]
ENSOARG00000009626	11.69907459	21.06078071	3.576386533	33.75690634	28.73043988	43.34286664	K06558 |0|oas:101121746 |MSR1; macrophage scavenger receptor 1; K06558 macrophage scavenger receptor 1 (A)	Macrophage scavenger receptor types I and II GN=MSR1 OS=Bos taurus (Bovine) PE=1 SV=1	PREDICTED: macrophage scavenger receptor types I and II isoform 1 [Ovis aries]
ENSOARG00000009762	6.127840818	4.683518846	2.455875242	9.677014649	9.103100404	13.40873882	--	Dihydrodiol dehydrogenase 3 OS=Bos taurus (Bovine) PE=2 SV=1	PREDICTED: dihydrodiol dehydrogenase 3-like [Ovis aries]
ENSOARG00000009963	2.192959404	1.922824841	0.519359545	6.820408815	4.91348855	5.463695561	K17310 |3.19906e-93 |oas:101121216 |serum amyloid A protein-like; K17310 serum amyloid A protein (A)	Amyloid protein A (Precursor) GN=SAA1 OS=Bos taurus (Bovine) PE=1 SV=2	serum amyloid A protein [Bubalus bubalis]
ENSOARG00000011217	5.321972229	6.357966671	1.655969652	11.49720041	9.858819699	14.28442636	K13783 |0|oas:101109494 |SLC37A2; solute carrier family 37 (glycerol-3-phosphate transporter), member 2; K13783 MFS transporter, OPA family, solute carrier family 37 (glycerol-3-phosphate transporter), member 1/2 (A)	Sugar phosphate exchanger 2 GN=SLC37A2 OS=Bos taurus (Bovine) PE=2 SV=1	PREDICTED: sugar phosphate exchanger 2 [Ovis aries]
ENSOARG00000011288	3.822256693	5.907407824	5.248680668	12.05024925	10.06275902	9.443023087	K05404 |0|chx:102171227 |TLR7; toll-like receptor 7; K05404 toll-like receptor 7 (A)	Toll-like receptor 9 (Precursor) GN=TLR9 OS=Sus scrofa (Pig) PE=2 SV=1	PREDICTED: toll-like receptor 7 isoform X1 [Capra hircus]
ENSOARG00000012307	1.781310087	3.142299727	0.934627269	7.261167162	5.061956052	7.456190044	--	Leucine-rich repeat-containing protein 25 (Precursor) GN=LRRC25 OS=Bos taurus (Bovine) PE=2 SV=1	PREDICTED: LOW QUALITY PROTEIN: leucine-rich repeat-containing protein 25 [Ovis aries]
ENSOARG00000012367	5.081457702	5.609270236	3.153254381	10.76418262	11.06912303	10.60698922	K06464 |0|oas:494433 |ITGB2, CD18; integrin, beta 2 (complement component 3 receptor 3 and 4 subunit); K06464 integrin beta 2 (A)	Integrin beta-2 (Precursor) GN=ITGB2 OS=Ovis aries (Sheep) PE=2 SV=1	integrin beta-2 precursor [Ovis aries]
ENSOARG00000012450	132.8153358	107.2708867	52.21277051	191.1758777	202.9396852	224.5781492	K13625 |4.45307e-125 |phd:102335976 |ferritin light chain-like; K13625 ferritin light chain (A)	Ferritin light chain GN=FTL OS=Bos taurus (Bovine) PE=2 SV=3	ferritin light chain [Bos taurus]
ENSOARG00000012748	27.26841681	46.12732385	21.82752755	80.74261748	95.39571486	88.00608533	--	M-beta (Precursor) GN=PMEL OS=Bos taurus (Bovine) PE=2 SV=2	PREDICTED: transmembrane glycoprotein NMB [Ovis aries]
ENSOARG00000013162	78.66086206	114.2772431	35.12873334	221.1218254	210.3862495	255.6831272	K01369 |0|oas:678680 |LGMN; legumain; K01369 legumain [EC:3.4.22.34] (A)	Legumain (Precursor) GN=LGMN OS=Bos taurus (Bovine) PE=1 SV=1	PREDICTED: legumain [Ovis aries]
ENSOARG00000013340	13.35621738	19.40617357	5.798781362	31.01386865	25.40558564	31.02653673	K05514 |2.17051e-44 |phd:102330755 |CCL26; chemokine (C-C motif) ligand 26; K05514 C-C motif chemokine, other (A)	C-C motif chemokine 26 (Precursor) GN=CCL26 OS=Canis familiaris (Dog) PE=3 SV=1	PREDICTED: c-C motif chemokine 26 [Ovis aries]
ENSOARG00000013445	3.769660409	2.986277426	1.001879507	6.847117429	6.702947055	9.868180117	K10656 |0|mcf:102121650 |MARCH1; membrane-associated ring finger (C3HC4) 1, E3 ubiquitin protein ligase; K10656 E3 ubiquitin-protein ligase MARCH1/8 [EC:6.3.2.19] (A)	E3 ubiquitin-protein ligase MARCH8 GN=MARCH8 OS=Bos taurus (Bovine) PE=2 SV=1	E3 ubiquitin-protein ligase MARCH1 [Pteropus alecto]
ENSOARG00000013948	4.242549823	3.094030783	4.937585067	0.610024142	1.784201955	1.905612297	K05175 |0|phd:102328547 |GABRA1; gamma-aminobutyric acid (GABA) A receptor, alpha 1; K05175 gamma-aminobutyric acid receptor subunit alpha (A)	Gamma-aminobutyric acid receptor subunit alpha-1 (Precursor) GN=GABRA1 OS=Bos taurus (Bovine) PE=1 SV=1	PREDICTED: gamma-aminobutyric acid receptor subunit alpha-1 isoform 4 [Ovis aries]
ENSOARG00000014339	370.09787	335.0560087	222.3738209	643.3529879	610.0144364	660.1791529	K00522 |3.73699e-106 |bom:102277133 |FTH1; ferritin, heavy polypeptide 1; K00522 ferritin heavy chain [EC:1.16.3.2] (A)	Ferritin heavy chain, N-terminally processed GN=FTH1 OS=Bos taurus (Bovine) PE=2 SV=3	PREDICTED: ferritin heavy chain [Bos mutus]
ENSOARG00000014440	2.686208646	2.055191655	1.743001177	8.193085693	7.686862951	7.213451515	K08069 |0|oas:101105005 |VNN1; vanin 1; K08069 pantetheine hydrolase [EC:3.5.1.92] (A)	Pantetheinase (Precursor) GN=VNN1 OS=Bos taurus (Bovine) PE=2 SV=1	PREDICTED: pantetheinase isoform 1 [Ovis aries]
ENSOARG00000014664	18.85919594	19.53768177	9.299113998	28.1955204	31.35370949	36.8179387	K01366 |0|oas:101108427 |CTSH; cathepsin H; K01366 cathepsin H [EC:3.4.22.16] (A)	Cathepsin H light chain (Precursor) GN=CTSH OS=Bos taurus (Bovine) PE=2 SV=1	PREDICTED: pro-cathepsin H [Ovis aries]
ENSOARG00000015082	122.8446698	120.728907	47.45720308	200.0636192	210.4396885	273.7924034	K01052 |0|oas:100145859 |LIPA; lipase A, lysosomal acid, cholesterol esterase (EC:3.1.1.13); K01052 lysosomal acid lipase/cholesteryl ester hydrolase [EC:3.1.1.13] (A)	Lysosomal acid lipase/cholesteryl ester hydrolase (Precursor) GN=LIPA OS=Macaca fascicularis (Crab-eating macaque) PE=2 SV=1	lysosomal acid lipase/cholesteryl ester hydrolase precursor [Ovis aries]
ENSOARG00000015263	173.0500573	220.6937075	61.56500466	382.0696052	373.1513633	457.9056218	K01363 |0|oas:780470 |CTSB; cathepsin B; K01363 cathepsin B [EC:3.4.22.1] (A)	Cathepsin B heavy chain (Precursor) GN=CTSB OS=Bos taurus (Bovine) PE=1 SV=5	PREDICTED: cathepsin B [Ovis aries]
ENSOARG00000015270	2.049022569	0.902171773	1.402506487	0.221106834	0.208681244	0.373252652	K12026 |0|oas:101120134 |TRIM56; tripartite motif containing 56; K12026 tripartite motif-containing protein 56 [EC:6.3.2.19] (A)	E3 ubiquitin-protein ligase TRIM56 GN=TRIM56 OS=Bos taurus (Bovine) PE=3 SV=1	PREDICTED: LOW QUALITY PROTEIN: E3 ubiquitin-protein ligase TRIM56 [Ovis aries]
ENSOARG00000015536	2.036002777	2.265893228	1.009544325	4.058719715	4.723582069	6.236122558	--	Protein O-linked-mannose beta-1,2-N-acetylglucosaminyltransferase 1 GN=POMGNT1 OS=Pongo abelii (Sumatran orangutan) PE=2 SV=1	PREDICTED: protein KIAA1199 homolog [Ovis aries]
ENSOARG00000016127	45.58312483	88.8006795	18.90531177	118.7221103	144.5968568	160.2856782	K08568 |0|oas:101101911 |cathepsin Z-like; K08568 cathepsin X [EC:3.4.18.1] (A)	Cathepsin Z (Precursor) GN=CTSZ OS=Bos taurus (Bovine) PE=2 SV=2	PREDICTED: cathepsin Z-like [Ovis aries]
ENSOARG00000017020	21.31976454	26.99365812	7.770026755	67.34632411	48.22976515	66.14823602	K06259 |0|oas:101102230 |platelet glycoprotein 4-like; K06259 CD36 antigen (A)	Platelet glycoprotein 4 GN=CD36 OS=Bos taurus (Bovine) PE=1 SV=5	PREDICTED: platelet glycoprotein 4-like [Ovis aries]
ENSOARG00000017314	1.844370475	2.443661484	0.393342424	4.227526125	3.954326334	4.227943653	K00710 |0|oas:101114859 |GALNT6; UDP-N-acetyl-alpha-D-galactosamine:polypeptide N-acetylgalactosaminyltransferase 6 (GalNAc-T6); K00710 polypeptide N-acetylgalactosaminyltransferase [EC:2.4.1.41] (A)	Polypeptide N-acetylgalactosaminyltransferase 6 GN=GALNT6 OS=Bos taurus (Bovine) PE=2 SV=1	PREDICTED: polypeptide N-acetylgalactosaminyltransferase 6 [Capra hircus]
ENSOARG00000017679	179.4950699	213.3954176	156.5935899	363.058181	452.0982129	569.3059391	K00522 |1.10771e-133 |oas:101105484 |ferritin heavy chain-like; K00522 ferritin heavy chain [EC:1.16.3.2] (A)	Ferritin heavy chain, N-terminally processed GN=FTH1 OS=Bos taurus (Bovine) PE=2 SV=3	PREDICTED: ferritin heavy chain-like [Ovis aries]
ENSOARG00000018673	17.7581956	24.57916875	9.817545411	31.33820864	49.66613612	55.29994187	K14379 |0|oas:100820744 |ACP5; acid phosphatase 5, tartrate resistant (EC:3.1.3.2); K14379 tartrate-resistant acid phosphatase type 5 [EC:3.1.3.2] (A)	Tartrate-resistant acid phosphatase type 5 (Precursor) GN=ACP5 OS=Sus scrofa (Pig) PE=1 SV=4	tartrate-resistant acid phosphatase type 5 precursor [Ovis aries]
ENSOARG00000019055	3.721860603	4.867734798	1.064155487	8.254057293	6.834899622	8.218539574	K01639 |0|oas:101104513 |NPL; N-acetylneuraminate pyruvate lyase (dihydrodipicolinate synthase); K01639 N-acetylneuraminate lyase [EC:4.1.3.3] (A)	N-acetylneuraminate lyase GN=NPL OS=Bos taurus (Bovine) PE=2 SV=1	PREDICTED: N-acetylneuraminate lyase isoform 1 [Ovis aries]
ENSOARG00000019424	6.157482964	10.21456239	4.703646766	23.63948151	23.32290137	25.52034128	K13867 |0|oas:101105078 |SLC7A7; solute carrier family 7 (amino acid transporter light chain, y+L system), member 7; K13867 solute carrier family 7 (L-type amino acid transporter), member 7 (A)	Large neutral amino acids transporter small subunit 2 GN=SLC7A8 OS=Pongo abelii (Sumatran orangutan) PE=2 SV=2	PREDICTED: Y+L amino acid transporter 1 isoform 1 [Ovis aries]
ENSOARG00000019463	6.566115342	9.096587093	1.974835136	18.50843398	13.81707174	22.1838928	K06489 |9.81815e-113 |oas:101112271 |CD53; CD53 molecule; K06489 CD53 antigen (A)	Leukocyte surface antigen CD53 GN=CD53 OS=Bos taurus (Bovine) PE=2 SV=1	CD53 molecule [Ovis aries]
ENSOARG00000019512	1.118294008	1.846332265	0.818428946	3.371887504	2.621860991	2.81561933	--	--	PREDICTED: DENN domain-containing protein 2D [Ovis aries]
ENSOARG00000019535	1.381593682	1.546451635	0.752931477	3.288630052	4.684619187	2.761888297	K12347 |0|oas:443365 |SLC11A1, NRAMP1; solute carrier family 11 (proton-coupled divalent metal ion transporters), member 1; K12347 natural resistance-associated macrophage protein (A)	Natural resistance-associated macrophage protein 1 GN=SLC11A1 OS=Ovis aries (Sheep) PE=2 SV=2	natural resistance-associated macrophage protein 1 [Ovis aries]
ENSOARG00000019610	1.971255143	4.161619135	0.815496823	7.775554032	6.710052888	10.54511747	--	--	PREDICTED: transmembrane protein C1orf162 homolog [Ovis aries]
ENSOARG00000019615	6.846834723	8.346089434	3.309882762	22.18984258	14.54363545	21.09159734	--	CMRF35-like molecule 9 (Precursor) GN=CD300LG OS=Bos taurus (Bovine) PE=2 SV=2	PREDICTED: protein ADORA3, isoform 3 isoform X6 [Bubalus bubalis]
ENSOARG00000020511	8.672169123	12.91921723	3.86350624	23.14237141	16.5288691	28.29719942	K10368 |0|oas:101101968 |CAPG; capping protein (actin filament), gelsolin-like; K10368 capping protein (actin filament), gelsolin-like (A)	Macrophage-capping protein GN=CAPG OS=Bos taurus (Bovine) PE=2 SV=1	PREDICTED: macrophage-capping protein isoform 1 [Ovis aries]
ENSOARG00000020515	17.1301183	9.322492754	9.02977391	28.08793192	30.03117246	27.89148114	K13915 |2.26784e-98 |oas:100049062 |LYZ; lysozyme (EC:3.2.1.17); K13915 lysozyme C [EC:3.2.1.17] (A)	Lysozyme C, non-stomach isozyme (Precursor) GN=LYS OS=Bos taurus (Bovine) PE=2 SV=4	lysozyme C precursor [Ovis aries]
ENSOARG00000020667	1.033350017	1.83079845	0.256494546	5.233404163	2.775388697	4.784554793	K06498 |0|oas:100192431 |FCGR1A; Fc fragment of IgG, high affinity Ia, receptor (CD64); K06498 high affinity immunoglobulin gamma Fc receptor I (A)	Low affinity immunoglobulin gamma Fc region receptor III (Precursor) GN=FCGR3 OS=Bos taurus (Bovine) PE=2 SV=1	high affinity immunoglobulin gamma Fc receptor I precursor [Ovis aries]
ENSOARG00000020861	153.8533569	198.5161922	73.77632488	308.405971	282.9449019	364.504451	K01368 |0|oas:780472 |CTSS; cathepsin S; K01368 cathepsin S [EC:3.4.22.27] (A)	Cathepsin S (Precursor) GN=CTSS OS=Bos taurus (Bovine) PE=1 SV=2	PREDICTED: cathepsin S isoform 1 [Ovis aries]
ENSOARG00000021138	0.047613159	0.06149374	0.051212948	1.265969154	0.800106162	1.077526967	K14538 |0|phd:102336213 |GNL3L; guanine nucleotide binding protein-like 3 (nucleolar)-like; K14538 nuclear GTP-binding protein (A)	Guanine nucleotide-binding protein-like 3-like protein GN=GNL3L OS=Bos taurus (Bovine) PE=2 SV=1	PREDICTED: guanine nucleotide-binding protein-like 3-like protein isoform X2 [Capra hircus]
Ovis_aries_newGene_12519	1.015276264	0.950662033	1.24219112	0.012051257	0.298567754	0.011966969	--	LINE-1 reverse transcriptase homolog OS=Nycticebus coucang (Slow loris) PE=3 SV=1	hypothetical protein M91_20604 [Bos mutus]
Ovis_aries_newGene_13826	3.301479169	3.748983373	2.813421785	1.802284195	0.46455905	0.496297476	--	--	PREDICTED: uncharacterized protein LOC101123329 [Ovis aries]
Ovis_aries_newGene_20349	0.024992076	0.075315269	0.008960533	0.166126331	0.223986418	0.416338777	--	--	hypothetical protein M91_10594, partial [Bos mutus]
Ovis_aries_newGene_24826	0.816063288	1.053968791	0.667098886	0.030997162	0.219414055	0.030780363	K10483 |1.12235e-172 |oas:101103558 |BTBD11; BTB (POZ) domain containing 11; K10483 BTB/POZ domain-containing protein 11 (A)	--	PREDICTED: LOW QUALITY PROTEIN: ankyrin repeat and BTB/POZ domain-containing protein BTBD11 [Ovis aries]
Ovis_aries_newGene_30814	0.236420178	0.244274672	0.050858942	1.885827322	0.847547173	1.605117936	K17914 |5.61341e-29 |bmor:101735908 |protein split ends-like; K17914 kinesin family member 13 (A)	--	Zinc finger protein 354A, partial [Bos mutus]
Ovis_aries_newGene_36166	0.01926277	0.024878412	0.020719131	0.969466299	0.604235367	0.690227498	--	--	reverse transcriptase-like [Bos taurus]
Ovis_aries_newGene_4861	0.455823621	1.070380152	0.832000707	0.10493273	0.123794752	0.039074556	K08111 |2.36467e-11 |bom:102284894 |GPC5; glypican 5; K08111 glypican 5 (A)	--	Spectrin beta chain, brain 2 [Bos mutus]

Table S3 Top20 Biological Process Terms of DE-mRNAs

GO.ID	Term	Annotated	Significant	Expected	KS
GO:0009887	organ morphogenesis	2508	5	9.22	3.10E-07
GO:0044763	single-organism cellular process	12940	51	47.59	1.40E-06
GO:0001501	skeletal system development	1683	6	6.19	3.20E-06
GO:0042742	defense response to bacterium	169	7	0.62	3.70E-06
GO:0050896	response to stimulus	9907	50	36.43	1.70E-05
GO:0045654	positive regulation of megakaryocyte differentiation	79	2	0.29	1.90E-05
GO:1901989	positive regulation of cell cycle phase transition	84	1	0.31	2.30E-05
GO:0006958	complement activation, classical pathway	28	2	0.1	2.70E-05
GO:0009888	tissue development	3162	9	11.63	4.50E-05
GO:0044765	single-organism transport	3913	26	14.39	0.00011
GO:0001818	negative regulation of cytokine production	152	6	0.56	0.00026
GO:0002376	immune system process	2537	28	9.33	0.00031
GO:0006950	response to stress	3422	29	12.58	0.00038
GO:0008206	bile acid metabolic process	49	1	0.18	0.00043
GO:0048513	organ development	5586	20	20.54	0.00055
GO:0019882	antigen processing and presentation	106	4	0.39	0.00066
GO:0035095	behavioral response to nicotine	11	1	0.04	0.0008
GO:0071384	cellular response to corticosteroid stimulus	28	1	0.1	0.00084
GO:0050718	positive regulation of interleukin-1 beta secretion	18	1	0.07	0.00087
GO:0016488	farnesol catabolic process	19	1	0.07	0.00098
GO:1900053	negative regulation of retinoic acid	19	1	0.07	0.0009

	biosynthetic process				8
GO:2000224	regulation of testosterone biosynthetic process	19	1	0.07	0.0009 8
GO:0022604	regulation of cell morphogenesis	449	1	1.65	0.0010 6
GO:0042448	progesterone metabolic process	27	1	0.1	0.0012
GO:2000353	positive regulation of endothelial cell apoptotic process	27	1	0.1	0.0012

Annotated: all genes annotated to the function of the number of genes; Significant: different expression gene annotated to the function of the number of genes; Expected: to the function of the number of different expression gene expectations; KS: p value of KS test , the smaller the KS value, indicating its enrichment is more significant.

Table S4 Top20 Cellular Component Terms of DE-mRNAs

GO.ID	Term	Annot	Signifi	Expe	KS

		ated	cant	cted	
GO:0044446	intracellular organelle part	7407	16	27.6	2.70E-05
GO:0005765	lysosomal membrane	98	2	0.37	8.60E-05
GO:0005789	endoplasmic reticulum membrane	601	1	2.24	0.00017
GO:0005576	extracellular region	3294	21	12.27	0.00042
GO:0005892	acetylcholine-gated channel complex	15	1	0.06	0.00043
GO:0005634	nucleus	6087	12	22.68	0.00238
GO:0005938	cell cortex	296	2	1.1	0.00252
GO:0044428	nuclear part	2871	5	10.7	0.00285
GO:0043234	protein complex	4474	15	16.67	0.00347
GO:0030670	phagocytic vesicle membrane	32	1	0.12	0.00644
GO:0097458	neuron part	985	3	3.67	0.00912
GO:0043005	neuron projection	663	2	2.47	0.01114
GO:0005829	cytosol	1316	7	4.9	0.01891
GO:0032991	macromolecular complex	5672	16	21.14	0.0196
GO:0012505	endomembrane system	2949	12	10.99	0.02332
GO:0034364	high-density lipoprotein particle	23	1	0.09	0.02334
GO:0044430	cytoskeletal part	1938	2	7.22	0.02398
GO:0043233	organelle lumen	2404	5	8.96	0.02521
GO:0070013	intracellular organelle lumen	2400	5	8.94	0.02752
GO:0031974	membrane-enclosed lumen	2468	5	9.2	0.03234

Table S5 Top20 Molecular Function Terms of DE-mRNAs

GO.ID	Term	Annotated	Significant	Expected	KS
GO:0005044	scavenger receptor activity	68	2	0.26	2.60E-07
GO:0015464	acetylcholine receptor activity	17	1	0.06	0.00028
GO:0004032	alditol:NADP+ 1-oxidoreductase activity	26	1	0.1	0.00032
GO:0047115	trans-1,2-dihydrobenzene-1,2-diol dehydrogenase activity	20	1	0.08	0.00058
GO:0005506	iron ion binding	212	5	0.81	0.00077
GO:0045703	ketoreductase activity	19	1	0.07	0.00084
GO:0047086	ketosteroid monooxygenase activity	19	1	0.07	0.00084

GO:0047020	15-hydroxyprostaglandin-D dehydrogenase (NADP+) activity	19	1	0.07	0.00084
GO:0047042	androsterone dehydrogenase (B-specific) activity	19	1	0.07	0.00084
GO:0047035	testosterone dehydrogenase (NAD+) activity	19	1	0.07	0.00084
GO:0047006	17-alpha,20-alpha-dihydroxypregn-4-en-3-one dehydrogenase activity	19	1	0.07	0.00084
GO:0045550	geranylgeranyl reductase activity	19	1	0.07	0.00084
GO:0047787	delta4-3-oxosteroid 5beta-reductase activity	19	1	0.07	0.00084
GO:0035410	dihydrotestosterone 17-beta-dehydrogenase activity	19	1	0.07	0.00084
GO:0018636	phenanthrene 9,10-monooxygenase activity	19	1	0.07	0.00084
GO:0047017	prostaglandin-F synthase activity	17	1	0.06	0.00177
GO:0036131	prostaglandin D2 11-ketoreductase activity	17	1	0.06	0.00177
GO:0004252	serine-type endopeptidase activity	158	1	0.6	0.00208
GO:0016787	hydrolase activity	2745	20	10.44	0.0024

Table S6 Top20 Cellular Component Terms of the target genes of DE-lncRNAs

GO.ID	Term	Annotated	Significant	Expected	KS
GO:0050896	response to stimulus	9907	5	4.48	6.50E-07
GO:0044763	single-organism cellular process	12940	6	5.86	1.50E-06
GO:0009888	tissue development	3162	1	1.43	4.40E-05
GO:0044765	single-organism transport	3913	1	1.77	9.70E-05
GO:0006950	response to stress	3422	2	1.55	0.00033
GO:0048513	organ development	5586	2	2.53	0.00039
GO:0044711	single-organism biosynthetic process	1265	1	0.57	0.00124

GO:0051716	cellular response to stimulus	7400	3	3.35	0.00154
GO:0006508	proteolysis	1261	2	0.57	0.00176
GO:0016043	cellular component organization	6252	3	2.83	0.00196
GO:0006810	transport	4832	1	2.19	0.00209
GO:0006957	complement activation, alternative pathway	16	1	0.01	0.00239
GO:0065008	regulation of biological quality	3641	3	1.65	0.00301
GO:0043170	macromolecule metabolic process	9613	6	4.35	0.00375
GO:0045934	negative regulation of nucleobase-containing compound metabolic process	1119	2	0.51	0.00388
GO:0006464	cellular protein modification process	3089	1	1.4	0.00474
GO:0006996	organelle organization	3561	2	1.61	0.0053
GO:0019538	protein metabolic process	5283	4	2.39	0.00546
GO:0002376	immune system process	2537	1	1.15	0.00862
GO:0030154	cell differentiation	4631	2	2.1	0.011
GO:0010466	negative regulation of peptidase activity	174	1	0.08	0.01208
GO:0048869	cellular developmental process	5001	2	2.26	0.01277

Significant: target gene of DE-lncRNAs that annotated to the function of the number of genes

Table S7 Top20 Biological Process Terms of the target genes of DE-lncRNAs

GO.ID	Term	Annotated	Significant	Expected	KS
GO:0044446	intracellular organelle part	7407	6	3.3	2.20E-05
GO:0005765	lysosomal membrane	98	1	0.04	0.00016
GO:0005576	extracellular region	3294	2	1.47	0.00079
GO:0005634	nucleus	6087	5	2.71	0.00218
GO:0044428	nuclear part	2871	4	1.28	0.00304
GO:0043234	protein complex	4474	4	1.99	0.00348
GO:0032991	macromolecular complex	5672	5	2.52	0.0173

					6
GO:0005829	cytosol	1316	1	0.59	0.01898
GO:0012505	endomembrane system	2949	2	1.31	0.02184
GO:0044430	cytoskeletal part	1938	1	0.86	0.02233
GO:0043233	organelle lumen	2404	3	1.07	0.02791
GO:0070013	intracellular organelle lumen	2400	3	1.07	0.03044
GO:0031300	intrinsic component of organelle membran...	167	0	0.07	0.03089
GO:0044422	organelle part	7655	6	3.41	0.03246
GO:0031974	membrane-enclosed lumen	2468	3	1.1	0.03541
GO:0036128	CatSper complex	14	1	0.01	0.03742
GO:0031981	nuclear lumen	2071	2	0.92	0.03743
GO:0015630	microtubule cytoskeleton	1336	1	0.59	0.04631
GO:0005694	chromosome	909	1	0.4	0.04749
GO:0034707	chloride channel complex	41	1	0.02	0.05312

Table S8 The pathway enrich in DE-mRNAs

#Kegg_pathway	**ko_id**	**Cluter_frequency**	**P-value**	**Corrected_P-value**
Lysosome	ko04142	14 out of 47 29.7872340425532%	4.24E-14	1.40E-12
Tuberculosis	ko05152	8 out of 47 17.0212765957447%	2.59E-05	0.000854
Mineral absorption	ko04978	5 out of 47 10.6382978723404%	3.46E-05	0.001141
Staphylococcus aureus infection	ko05150	5 out of 47 10.6382978723404%	0.00011	0.003615
Pertussis	ko05133	5 out of 47 10.6382978723404%	0.00011 6	0.003835
Phagosome	ko04145	7 out of 47 14.8936170212766%	0.00017 8	0.005882
Osteoclast differentiation	ko04380	5 out of 47	0.0007	0.025813

		10.6382978723404%	82	
Complement and coagulation cascades	ko04610	3 out of 47 6.38297872340426%	0.0113 77	0.375438
Leishmaniasis	ko05140	3 out of 47 6.38297872340426%	0.0130 24	0.429805
Legionellosis	ko05134	3 out of 47 6.38297872340426%	0.0143 45	0.473391
Hematopoietic cell lineage	ko04640	3 out of 47 6.38297872340426%	0.0177 14	0.584572
Prion diseases	ko05020	2 out of 47 4.25531914893617%	0.0186 36	0.614976
Fc gamma R-mediated phagocytosis	ko04666	3 out of 47 6.38297872340426%	0.0192 82	0.636317
Antigen processing and presentation	ko04612	3 out of 47 6.38297872340426%	0.0244 36	0.8064
Nicotine addiction	ko05033	2 out of 47 4.25531914893617%	0.0286 33	0.944905
Natural killer cell mediated cytotoxicity	ko04650	3 out of 47 6.38297872340426%	0.0309 56	1
Systemic lupus erythematosus	ko05322	3 out of 47 6.38297872340426%	0.0517 47	1
Malaria	ko05144	2 out of 47 4.25531914893617%	0.0550 21	1
PPAR signaling pathway	ko03320	2 out of 47 4.25531914893617%	0.0662 72	1
Rheumatoid arthritis	ko05323	2 out of 47 4.25531914893617%	0.1438 66	1
Rap1 signaling pathway	ko04015	3 out of 47 6.38297872340426%	0.1460 46	1
Regulation of actin cytoskeleton	ko04810	3 out of 47 6.38297872340426%	0.1517 28	1
Protein digestion and absorption	ko04974	2 out of 47 4.25531914893617%	0.1627 86	1
Sphingolipid signaling pathway	ko04071	2 out of 47 4.25531914893617%	0.1670 53	1
Leukocyte transendothelial migration	ko04670	2 out of 47 4.25531914893617%	0.1691 93	1
Chagas disease (American trypanosomiasis)	ko05142	2 out of 47 4.25531914893617%	0.1691 93	1
Amoebiasis	ko05146	2 out of 47 4.25531914893617%	0.1734 9	1
Neuroactive ligand-receptor interaction	ko04080	3 out of 47 6.38297872340426%	0.2505 28	1
Influenza A	ko05164	2 out of 47	0.2979	1

		4.25531914893617%	94	
Transcriptional misregulation in cancer	ko05202	2 out of 47 4.25531914893617%	0.3114 32	1
Cell adhesion molecules (CAMs)	ko04514	2 out of 47 4.25531914893617%	0.3270 52	1
Viral carcinogenesis	ko05203	2 out of 47 4.25531914893617%	0.4183 88	1
PI3K-Akt signaling pathway	ko04151	2 out of 47 4.25531914893617%	0.6561 37	1

Table S9 The pathway enrich in DE-lncRNAs

#Kegg_pathway	**ko_id**	**Cluter_frequency**	**P-value**	**Corrected_P-value**
Spliceosome	ko03040	2 out of 6 33.3333333333333%	0.007233	0.13743
Other glycan degradation	ko00511	1 out of 6 16.6666666666667%	0.020597	0.391341
Aminoacyl-tRNA biosynthesis	ko00970	1 out of 6 16.6666666666667%	0.036371	0.691052
Sphingolipid metabolism	ko00600	1 out of 6 16.6666666666667%	0.037117	0.705223
Lysine degradation	ko00310	1 out of 6 16.6666666666667%	0.051197	0.972741
Complement and coagulation cascades	ko04610	1 out of 6 16.6666666666667%	0.058538	1
Staphylococcus aureus infection	ko05150	1 out of 6 16.6666666666667%	0.060001	1

RNA degradation	ko03018	1 out of 6 16.6666666666667%	0.060001	1
Legionellosis	ko05134	1 out of 6 16.6666666666667%	0.063649	1
Estrogen signaling pathway	ko04915	1 out of 6 16.6666666666667%	0.075964	1
Antigen processing and presentation	ko04612	1 out of 6 16.6666666666667%	0.077404	1
Lysosome	ko04142	1 out of 6 16.6666666666667%	0.095247	1
Toxoplasmosis	ko05145	1 out of 6 16.6666666666667%	0.100895	1
Measles	ko05162	1 out of 6 16.6666666666667%	0.103006	1
Influenza A	ko05164	1 out of 6 16.6666666666667%	0.131439	1
Protein processing in endoplasmic reticulum	ko04141	1 out of 6 16.6666666666667%	0.136217	1
Epstein-Barr virus infection	ko05169	1 out of 6 16.6666666666667%	0.15645	1
Endocytosis	ko04144	1 out of 6 16.6666666666667%	0.168398	1
MAPK signaling pathway	ko04010	1 out of 6 16.6666666666667%	0.186704	1